Nonlinear Dyn (2023) 111:17317–17336
https://doi.org/10.1007/s11071-023-08780-5

ORIGINAL PAPER

# Adaptive observer for ODE-PDE cascade systems subject to nonlinear dynamics and uncertain parameters

**Chunting Ji · Zhengqiang Zhang**

Received: 24 February 2023 / Accepted: 17 July 2023 / Published online: 4 August 2023


**Abstract** In this article, state and parameter estimation problems are investigated for ODE-PDE coupled systems, for which the parabolic PDE sensor includes nonlinear dynamics and parameter uncertainty. The major difficulty we face is that the link point among the ODE part and the PDE part is not convenient to measurable. For this reason, the objective of this paper is to build an adaptive observer to provide online estimates of states and unknown parameters on the basis that only boundary state is available for measurement. First of all, the observer error system is converted to a tractable target error system by applying the decoupling transformation. Then, the least-squares parameter adaptive law is built. Under an ad hoc persistent excitation condition, the exponentially decaying of the observer error system is demonstrated by applying Lyapunov–Krasovskii functional. Finally, the effectiveness of the theoretical results is confirmed by a simulation example.

**Keywords** ODE-PDE cascade systems · Adaptive observer · Nonlinear dynamics · Uncertainty

Chunting Ji and Zhengqiang Zhang have contributed equally to this work.

C. Ji · Z. Zhang (✉)
School of Engineering, Qufu Normal University, Rizhao 276826, Shandong, China
e-mail: qufuzzq@126.com

C. Ji
e-mail: qfjct@sina.com

## 1 Introduction

It is well-known that the state observer design for finite-dimensional system has been greatly developed in the last thirty years. Since partial differential equations (PDEs) can more accurately describe various phenomena in nature, such as fluid mechanics, heat conduction, electromagnetic field, wave phenomena, quantum mechanics and so on. Recently, people have gradually paid attention to state observer design for infinite-dimensional system described by PDEs. In this respect, Smyshlyaev and Krstic did some pioneering work. In Ref. [1], they constructed the collocated and anti-collocated backstepping observers for parabolic partial integro-differential equations (PIDEs).

As far as we know, the ODE plant with the PDE actuator dynamics (namely, PDE-ODE cascade systems) have abundant application, such as: coupled electromagnetic, chemical reactions and mechanical, etc. Thus, there are also many meaningful results for the observer design of PDE-ODE cascade systems. References [2] and [3] established the anti-collocated observer for PDE-ODE cascade systems with constant coefficient and spatially varying coefficient, respectively. In Ref. [4], a Luenberger observer was designed for nonlinear multivariable systems with diffusion PDE-governed sensor dynamics. In Ref. [5], a collocated observer was presented for the first-order hyperbolic PDE-ODE cascade systems using the Volterra integral transformation. Then, a novel anti-collocated

observer was proposed for under-actuated PDE-ODE coupled system in Refs. [6] and [7], respectively. However, in practical applications, the ODE-PDE cascade systems cannot be ignored, where the ODE and the PDE stand for the plant and the sensor, respectively. The observer design of the ODE plant with diffusive sensor dynamics was presented for the first time in Ref. [8]. Then, Ahmed-Ali et al. extended the observer design approach to the nonlinear ODEs with parabolic and hyperbolic sensors in Refs. [9] and [10], respectively, where the nonlinear dynamics have a lower triangular structure. The authors of Ref. [11] developed a sample boundary observer for strict-feedback nonlinear system with heat PDE sensor. Later, sample boundary observer was built for linear ODEs with nonlinear parabolic PDE sensor in Ref. [12]. In Ref. [13], the authors constructed a Luenberger-type observer for the Stefan system and applied the results to polar ice dynamics model and charging and discharging in lithium-ion batteries model.

It is worth emphasizing that most of the above systems require the mathematical model to be fully known. In fact, due to the working mechanism of the controlled object may not be clear, the measurement accuracy may not be accurate or other influences, the system inevitably has a variety of uncertainties. It is well known that adaptive technology is an effective method to eliminate the influence of unknown parameters on the system, see Ref. [14]. Therefore, there is also great interest in the design of adaptive observers for scalar PDE and coupled systems with uncertain parameters. In Refs. [15–17], by utilizing backstepping-like transformations, the anti-collocated adaptive observers were established for scalar parabolic equation and fully coupled parabolic equations with uncertain parameters. Adaptive boundary observers were also designed for transport and wave PDEs with unknown parameters in Refs. [18] and [19], respectively. Meanwhile, the authors of Refs. [20] and [21] proposed a continuous observer and a sampled-data observer for the linear ODE-heat PDE coupled systems subject to parameter uncertainty, respectively.

From the above discussion, it can be found that there are three main constraints in the existing results for ODE-PDE cascade systems: (i) The uncertainty of the system only acts on its domain, and the case where the boundary is also affected by the uncertainty is not considered; (ii) When the parameter uncertainty is present, the PDE sensor is a linear system, while most phenomena in nature are nonlinear; (iii) When the Lipschitz nonlinearity is involved, the Lipschitz coefficient and the PDE domain length are not permitted to be concurrently large.

In this paper, our goal is to break through constraints (i) and (ii) and relax constraint (iii): ① Considering that both the boundary and the domain are affected by parameter uncertainty; ② Considering that the PDE sensor contains nonlinearity; ③ Even if the PDE domain length and the Lipschitz coefficient cannot be simultaneously large, with the increase of diffusion coefficient, the value range of the PDE domain length and the Lipschitz coefficient becomes larger. The novelty of this paper includes:

- A novel backstepping-like transformation is applied to decouple unknown states and parameters.
- A least-squares type update law is designed to accurately estimate the decoupled unknown states and parameters online.
- We relax the condition of Ref. [12, Theorem 1].

We proceed as follows. Section 2 proposes the main issues and presents some necessary information. In Sect. 3, combining the decoupling transformation and least-squares type parameter update law, an anti-collocated adaptive state observer is built. Then, the exponential stability of the observer error system is analyzed in Sect. 4. Finally, a simulation example is utilized to confirm the validity of the theoretical method in Sect. 5.

***Notation.*** Throughout the text, $\mathcal{R}^n$ and $\mathcal{R}^{n\times m}$ are $n$ dimensional real space and $n\times m$ real matrices, respectively. The symbol $\|\cdot\|$ denotes the corresponding Euclidean norm. $\mathcal{L}^2(0,\ell)$ represents the Hilbert space of square integrable function $p:[0,\ell]\to\mathcal{R}$, its $\mathcal{L}^2$-norm is given by $\|p\|_2=\sqrt{\int_0^\ell p^2(\xi)d\xi}$. Here, $\ell>0$ is the PDE domain length. $\mathcal{H}^i(0,\ell)$ is the Sobolev space of absolutely continuous functions $p:[0,\ell]\to\mathcal{R}$ with $\mathrm{d}^i p/\mathrm{d}\sigma^i\in\mathcal{L}^2(0,\ell)$. For a scalar function $q\in\mathcal{H}^1(0,\ell)$ with $q(0)=0$ or $q(\ell)=0$, it is easy to give that the following Wirtinger's inequalities (see, e.g., Refs. [22, Sect. 7.6] and [23])

$$\int_0^\ell q^2(\sigma,t)d\sigma\le\frac{4\ell^2}{\pi^2}\int_0^\ell q_\sigma^2(\sigma,t)d\sigma, \tag{1a}$$

$$\max_{0\le\sigma\le\ell}q^2(\sigma,t)\le\ell\int_0^\ell q_\sigma^2(\sigma,t)d\sigma \tag{1b}$$

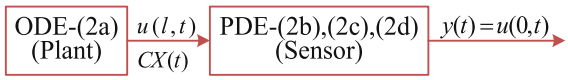


**Fig. 1** The block diagram of the plant consisting of (2a)–(2d)

For simplicity, we sometimes omit the time variable $t$.

## 2 Problem formulation

In the present work, we are devoted to investigate the following ODE-PDE coupled systems subject to unknown parameters and nonlinear dynamics. The block diagram of the system structure is displayed in Fig. 1.

$$\dot{X}(t) = AX(t) + \phi_1(t)\rho_1, \tag{2a}$$

$$u_t(\sigma,t) = hu_{\sigma\sigma}(\sigma,t) + g(u(\sigma,t),\sigma,t) + \phi_2(\sigma,t)\rho_2, \tag{2b}$$

$$u_\sigma(0,t) = \phi_3(t)\rho_3, \tag{2c}$$

$$u(\ell,t) = CX(t) + \phi_4(t)\rho_4, \tag{2d}$$

where $X(t) \in \mathcal{R}^n$ and $u(\sigma,t) \in \mathcal{R}$ with initial data $X(0) = X_0$ and $u(\sigma,0) = u_0(\sigma)$ denote ODE and PDE states, respectively. Here, $h > 0$ is called the diffusion coefficient. $A \in \mathcal{R}^{n\times n}$, $C^T \in \mathcal{R}^n$ are known constant matrices and satisfy the pair $(A, C)$ is observable. $\phi_1(t) \in \mathcal{C}^1([0,+\infty) : \mathcal{R}^{n\times m_1})$, $\phi_2(\sigma,t) \in \mathcal{C}^1([0,\ell]\times[0,+\infty) : \mathcal{R}^{1\times m_2})$, $\phi_3(t) \in \mathcal{C}^1([0,+\infty) : \mathcal{R}^{1\times m_3})$ and $\phi_4(t) \in \mathcal{C}^1([0,+\infty) : \mathcal{R}^{1\times m_4})$ are known bounded functions. $\rho_i \in \mathcal{R}^{m_i}(i = 1,2,3,4)$ are unknown constant parameter vectors. We suppose that $m = m_1+m_2+m_3+m_4$. In addition, $g(u(\sigma,t),\sigma,t) \in \mathcal{C}^1(\mathcal{R}\times[0,\ell]\times[0,+\infty) : \mathcal{R})$ is a known mapping, it does not have any special form but its derivative is bounded with respect to its first argument, namely, for $\forall(u,\sigma,t) \in \mathcal{R}\times[0,\ell]\times[0,+\infty)$, there has a constant $\beta > 0$ such that

$$|g_u(u,\sigma,t)| \le \beta. \tag{3}$$

The main aim of this note is to build an adaptive boundary observer that can offer accurate online estimates of the system states $X(t), u(\sigma,t)$ and unknown parameter vectors $\rho_i(i = 1,2,3,4)$ only when the boundary state $u(0,t)$ is continuous measurable.

*Remark 1* In this note, the uncertain quantity and nonlinear dynamics in (2a)–(2d) constitute new features compared to Ref. [8] where $\rho_i = 0(i = 1,2,3,4)$ and $g = 0$. On the other hand, if $g$, $\rho_i(i = 3,4)$ are all set to zero, the system (2a)–(2d) boils down to the system consisting of (2) and (3a)–(3b) in Ref. [20].

## 3 Adaptive observer design

### 3.1 Observer construction

In this part, we only use the boundary output measurable signal $y(t) = u(0,t)$ to construct the following the anti-collocated observer, which is a copy of the ODE-PDE cascade systems (2a)–(2d)

$$\dot{\hat{X}}(t) = A\hat{X}(t) + \phi_1(t)\hat{\rho}_1(t) - L\big(\hat{u}(0,t) - y(t)\big) + v_1(t), \tag{4a}$$

$$\hat{u}_t(\sigma,t) = h\hat{u}_{\sigma\sigma}(\sigma,t) + g(\hat{u}(\sigma,t),\sigma,t) + \phi_2(\sigma,t)\hat{\rho}_2(t) - p(\sigma)\big(\hat{u}(0,t) - y(t)\big) + v_2(\sigma,t), \tag{4b}$$

$$\hat{u}_\sigma(0,t) = \phi_3(t)\hat{\rho}_3(t), \tag{4c}$$

$$\hat{u}(\ell,t) = C\hat{X}(t) + \phi_4(t)\hat{\rho}_4(t), \tag{4d}$$

where $\hat{X}(t)$ and $\hat{u}(\sigma,t)$ with initial conditions $\hat{X}(0) = \hat{X}_0$ and $\hat{u}(\sigma,0) = \hat{u}_0(\sigma)$ are the estimates of the states $X(t)$ and $u(\sigma,t)$, respectively. $\hat{\rho}_i(t)$ with initial data $\hat{\rho}_i(0) = \hat{\rho}_{i0}$ are the estimates of unknown parameter vectors $\rho_i(i = 1,2,3,4)$, respectively. $L \in \mathcal{R}^n$ and $p(\sigma) \in \mathcal{R}$ are the observer gains. Besides, $v_1(t)$ and $v_2(\sigma,t)$ are added functions to be defined later.

Without loss of generality, let $\tilde{X}(t) = \hat{X}(t) - X(t)$, $\tilde{u}(\sigma,t) = \hat{u}(\sigma,t) - u(\sigma,t)$ and $\tilde{\rho}_i(t) = \hat{\rho}_i(t) - \rho_i(i = 1,2,3,4)$, then subtracting (4a)–(4d) into (2a)–(2d), we get

$$\dot{\tilde{X}}(t) = A\tilde{X}(t) + \phi_1(t)\tilde{\rho}_1(t) - L\tilde{u}(0,t) + v_1(t), \tag{5a}$$

$$\tilde{u}_t(\sigma,t) = h\tilde{u}_{\sigma\sigma}(\sigma,t) + \tilde{g}(\sigma,t) + \phi_2(\sigma,t)\tilde{\rho}_2(t) - p(\sigma)\tilde{u}(0,t) + v_2(\sigma,t), \tag{5b}$$

$$\tilde{u}_\sigma(0,t) = \phi_3(t)\tilde{\rho}_3(t), \tag{5c}$$

$$\tilde{u}(\ell,t) = C\tilde{X}(t) + \phi_4(t)\tilde{\rho}_4(t), \tag{5d}$$

where

$$\tilde{g}(\sigma,t)=g(\hat{u}(\sigma,t),\sigma,t)-g(u(\sigma,t),\sigma,t).$$

### 3.2 Decoupling transformation

In this section, we first adopt the following backstepping-like transformation to decouple the unknown states and parameters

$$Z(t)=\tilde{X}(t)-\sum_{i=1}^{4}\lambda_{1i}(t)\tilde{\rho}_i(t), \tag{6a}$$

$$w(\sigma,t)=\tilde{u}(\sigma,t)-C\Omega(\sigma)\Omega^{-1}(\ell)\tilde{X}(t)-\sum_{i=1}^{4}\lambda_{2i}(\sigma,t)\tilde{\rho}_i(t), \tag{6b}$$

for any $(\sigma,t)\in[0,\ell]\times[0,+\infty)$. Here, $\lambda_{1i}(t)\in\mathcal{R}^{n\times m_i}$ and $\lambda_{2i}(\sigma,t)\in\mathcal{R}^{1\times m_i}$ $(i=1,2,3,4)$ are auxiliary state matrices and vectors, respectively. The matrix function $\Omega(\sigma)\in\mathcal{R}^{n\times n}$ is determined by the following ODEs:

$$\frac{\mathrm{d}^2\Omega}{\mathrm{d}\sigma^2}(\sigma)=\frac{1}{h}\Omega(\sigma)A,\quad \frac{\mathrm{d}\Omega}{\mathrm{d}\sigma}(0)=0,\quad \Omega(0)=I. \tag{7}$$

It is important to note, the matrix function $\Omega(\sigma)$ has played a crucial role in the observer design and its properties are given in Appendix A. From (6b), we found that $\Omega(\ell)$ needs to be invertible, which means that it is necessary to impose a constraint on the matrix $A$. As described in Ref. [9], if the matrix $A$ is nilpotent, that is, $A^n=0$, thus $\Omega(\ell)$ is invertible. It should be pointed out that this property also holds for other classes of matrix $A$.

Next, we transform the observer error system (5a)–(5d) into an easy-to-handle target error system by the decoupling transformation (6a)–(6b). To this end, differentiating (6a) with respect to $t$ and using (5a), we deduce

$$\begin{aligned}\dot{Z}(t)&=\dot{\tilde{X}}(t)-\sum_{i=1}^{4}\dot{\lambda}_{1i}(t)\tilde{\rho}_i(t)-\sum_{i=1}^{4}\lambda_{1i}(t)\dot{\tilde{\rho}}_i(t)\\&=A\tilde{X}(t)+\phi_1(t)\tilde{\rho}_1(t)-L\tilde{u}(0,t)+v_1(t)\\&\quad-\sum_{i=1}^{4}\dot{\lambda}_{1i}(t)\tilde{\rho}_i(t)-\sum_{i=1}^{4}\lambda_{1i}(t)\dot{\tilde{\rho}}_i(t).\end{aligned} \tag{8}$$

Selecting $v_1(t)=\sum_{i=1}^{4}\lambda_{1i}(t)\dot{\hat{\rho}}_i(t)$, it follows from (6a) and (7) that

$$\begin{aligned}\dot{Z}(t)=&\big(A-LC\Omega^{-1}(\ell)\big)Z(t)-Lw(0,t)+\phi_1(t)\tilde{\rho}_1(t)\\&-L\sum_{i=1}^{4}\lambda_{2i}(0,t)\tilde{\rho}_i(t)-\sum_{i=1}^{4}\dot{\lambda}_{1i}(t)\tilde{\rho}_i(t)\\&+\big(A-LC\Omega^{-1}(\ell)\big)\sum_{i=1}^{4}\lambda_{1i}(t)\tilde{\rho}_i(t).\end{aligned} \tag{9}$$

By eliminating the terms with $\tilde{\rho}_i(t)(i=1,2,3,4)$ in the above equality, we can obtain that the auxiliary state matrices $\lambda_{1i}(t)(i=1,2,3,4)$ satisfy

$$\begin{cases}\dot{\lambda}_{11}(t)=\big(A-LC\Omega^{-1}(\ell)\big)\lambda_{11}(t)+\phi_1(t)-L\lambda_{21}(0,t),\\ \dot{\lambda}_{12}(t)=\big(A-LC\Omega^{-1}(\ell)\big)\lambda_{12}(t)-L\lambda_{22}(0,t),\\ \dot{\lambda}_{13}(t)=\big(A-LC\Omega^{-1}(\ell)\big)\lambda_{13}(t)-L\lambda_{23}(0,t),\\ \dot{\lambda}_{14}(t)=\big(A-LC\Omega^{-1}(\ell)\big)\lambda_{14}(t)-L\lambda_{24}(0,t).\end{cases} \tag{10}$$

Substituting (10) into (9), we have

$$\dot{Z}(t)=\big(A-LC\Omega^{-1}(\ell)\big)Z(t)-Lw(0,t), \tag{11}$$

where $A-LC\Omega^{-1}(\ell)$ is a Hurwitz matrix.

*Remark 2* Utilizing the property $(c)$ of Appendix A, we infer that the equality $A=\Omega(\ell)A\Omega^{-1}(\ell)$ holds. In particular, we get

$$\begin{aligned}A-LC\Omega^{-1}(\ell)&=\Omega(\ell)A\Omega^{-1}(\ell)-LC\Omega^{-1}(\ell)\\&=\Omega(\ell)\big(A-\Omega^{-1}(\ell)LC\big)\Omega^{-1}(\ell),\end{aligned}$$

which implies that matrices $A-LC\Omega^{-1}(\ell)$ and $A-\Omega^{-1}(\ell)LC$ are similar and therefore have equivalent eigenvalues. Since the pair $(A,C)$ is observable, one has a suitable vector $L$ such that $A-\Omega^{-1}(\ell)LC$ is a Hurwitz matrix, so $A-LC\Omega^{-1}(\ell)$ is also a Hurwitz matrix.

Next, taking the time derivative of (6b) and utilizing (5a)–(5b), we obtain

$$\begin{aligned}w_t(\sigma,t)&=\tilde{u}_t(\sigma,t)-C\Omega(\sigma)\Omega^{-1}(\ell)\dot{\tilde{X}}(t)\\&\quad-\sum_{i=1}^{4}\lambda_{2i,t}(\sigma,t)\tilde{\rho}_i(t)-\sum_{i=1}^{4}\lambda_{2i}(\sigma,t)\dot{\tilde{\rho}}_i(t)\\&=h\tilde{u}_{\sigma\sigma}(\sigma,t)+\tilde{g}(\sigma,t)\end{aligned}$$

$$
\begin{aligned}
&+\phi_2(\sigma,t)\tilde{\rho}_2(t)-p(\sigma)\tilde{u}(0,t)+v_2(\sigma,t)\\
&-C\Omega(\sigma)\Omega^{-1}(\ell)\big(A\tilde{X}(t)+\phi_1(t)\tilde{\rho}_1(t)\\
&-L\tilde{u}(0,t)+v_1(t)\big)\\
&-\sum_{i=1}^{4}\lambda_{2i,t}(\sigma,t)\tilde{\rho}_i(t)-\sum_{i=1}^{4}\lambda_{2i}(\sigma,t)\dot{\tilde{\rho}}_i(t).
\end{aligned}
\tag{12}
$$

Similarly, we choose

$$
v_2(\sigma,t)=C\Omega(\sigma)\Omega^{-1}(\ell)v_1(t)+\sum_{i=1}^{4}\lambda_{2i}(\sigma,t)\dot{\hat{\rho}}_i(t).
\tag{13}
$$

Substituting (6b) and (13) into (12), it follows that

$$
\begin{aligned}
w_t(\sigma,t)=&\,hw_{\sigma\sigma}(\sigma,t)+\tilde{g}(\sigma,t)\\
&+hC\frac{\mathrm{d}^2\Omega}{\mathrm{d}\sigma^2}(\sigma)\Omega^{-1}(\ell)\tilde{X}(t)\\
&-C\Omega(\sigma)\Omega^{-1}(\ell)A\tilde{X}(t)+\phi_2(\sigma,t)\tilde{\rho}_2(t)\\
&-\big(p(\sigma)-C\Omega(\sigma)\Omega^{-1}(\ell)L\big)\tilde{u}(0,t)\\
&-C\Omega(\sigma)\Omega^{-1}(\ell)\phi_1(t)\tilde{\rho}_1(t)\\
&+\sum_{i=1}^{4}\big(h\lambda_{2i,\sigma\sigma}(\sigma,t)-\lambda_{2i,t}(\sigma,t)\big)\tilde{\rho}_i(t).
\end{aligned}
\tag{14}
$$

By eliminating the last four terms, it is easy to give that the trajectories of the auxiliary state matrices $\lambda_{2i}(\sigma,t)(i=1,2,3,4)$, respectively, satisfy

$$
\begin{cases}
\lambda_{21,t}(\sigma,t)=h\lambda_{21,\sigma\sigma}(\sigma,t)-C\Omega(\sigma)\Omega^{-1}(\ell)\phi_1(t),\\
\lambda_{22,t}(\sigma,t)=h\lambda_{22,\sigma\sigma}(\sigma,t)+\phi_2(\sigma,t),\\
\lambda_{23,t}(\sigma,t)=h\lambda_{23,\sigma\sigma}(\sigma,t),\\
\lambda_{24,t}(\sigma,t)=h\lambda_{24,\sigma\sigma}(\sigma,t),
\end{cases}
\tag{15}
$$

and the observer gain $p(\sigma)$ satisfies

$$
p(\sigma)=C\Omega(\sigma)\Omega^{-1}(\ell)L.
\tag{16}
$$

Inserting (15) and (16) to (14), then using (7) and the property $(b)$ of Appendix A, it is easy to get

$$
w_t(\sigma,t)=hw_{\sigma\sigma}(\sigma,t)+\tilde{g}(\sigma,t).
\tag{17}
$$

Then, it follows from (6b) that

$$
\begin{cases}
w_\sigma(0,t)=\tilde{u}_\sigma(0,t)-\sum_{i=1}^{4}\lambda_{2i,\sigma}(0,t)\tilde{\rho}_i(t),\\
w(\ell,t)=\tilde{u}(\ell,t)-C\tilde{X}(t)-\sum_{i=1}^{4}\lambda_{2i}(\ell,t)\tilde{\rho}_i(t).
\end{cases}
\tag{18}
$$

Choosing

$$
\begin{cases}
\lambda_{21,\sigma}(0,t)=0, & \lambda_{22,\sigma}(0,t)=0,\\
\lambda_{23,\sigma}(0,t)=\phi_3(t), & \lambda_{24,\sigma}(0,t)=0,\\
\lambda_{21}(\ell,t)=0, & \lambda_{22}(\ell,t)=0,\\
\lambda_{23}(\ell,t)=0, & \lambda_{24}(\ell,t)=\phi_4(t),
\end{cases}
\tag{19}
$$

and utilizing (4c)–(4d), we can obtain that the following boundary conditions are associated to (17)

$$
\begin{cases}
w_\sigma(0,t)=0,\\
w(\ell,t)=0.
\end{cases}
\tag{20}
$$

In this way, the target error system consisting of (11), (17) and (20) is established.

*Remark 3* The backstepping-like transformation described by (6a)–(6b) is a pivotal feature of the observer design and analysis. It is partly motivated by the previous finite- or infinite-dimensional transformations, but is also a generalization. In fact, the finite-dimensional transformation in Ref. [24] is achieved by taking $\lambda_{1i}(t)(i=2,3,4)$ be zero and deleting (6b), which can be utilized to adaptive observer design for ODEs. Similarly, the infinite-dimensional transformation in Ref. [8] is achieved by taking $\lambda_{2i}(i=1,2,3,4)$ be zero and deleting (6a), which can be utilized to non-adaptive observer design for ODE-PDEs. In addition, the transformation in [20] can be regarded as a particular case of (6a)-(6b) by taking $\lambda_{13}(t)$, $\lambda_{14}(t)$ and $\lambda_{23}(\sigma,t)$, $\lambda_{24}(\sigma,t)$ be zero. It is worthy mentioning that the new transformation (6a)–(6b) features a coupling among the finite- and infinite-dimensional transformations. This coupling is part of the novelty of the present transformation, which can be used to decouple unknown states and parameters.

### 3.3 Parameter adaptive law

In this section, we design the ensuing parameter adaptive law to online accurately estimate unknown parameters by utilizing the known signals $u(0,t)$ and $\phi_1(t)$, $\phi_2(\sigma,t)$, $\phi_3(t)$, $\phi_4(t)$

$$\dot{\hat{\rho}}(t) = -Q(t)\Gamma(t)\tilde{u}(0,t), \tag{21a}$$

$$\dot{Q}(t) = \alpha Q(t) - Q(t)\Gamma(t)\Gamma^T(t)Q(t), \tag{21b}$$

where $\hat{\rho}(t) = [\hat{\rho}_1^T(t), \hat{\rho}_2^T(t), \hat{\rho}_3^T(t), \hat{\rho}_4^T(t)]^T \in \mathcal{R}^m$ with the initial data $\hat{\rho}(0) = \rho_0$ and $Q(t) \in \mathcal{R}^{m\times m}$ is a matrix gain with the initial value $Q(0) = Q_0 = Q_0^T > 0$. In addition, $\alpha > 0$ is a scalar to be set later, and

$$\Gamma(t) = \begin{pmatrix} \left(C\Omega^{-1}(\ell)\lambda_{11}(t) + \lambda_{21}(0,t)\right)^T \\ \left(C\Omega^{-1}(\ell)\lambda_{12}(t) + \lambda_{22}(0,t)\right)^T \\ \left(C\Omega^{-1}(\ell)\lambda_{13}(t) + \lambda_{23}(0,t)\right)^T \\ \left(C\Omega^{-1}(\ell)\lambda_{14}(t) + \lambda_{24}(0,t)\right)^T \end{pmatrix}. \tag{22}$$

Next, we suppose the ensuing persistent excitation (PE) condition to be true.

**PE Assumption.** The vector signal $\Gamma(t)$ defined by (22) is assumed to be persistently exciting, i.e., for some positive constants $\tau$ and $\epsilon_0$, there exists

$$\int_t^{t+\tau} \Gamma(s)\Gamma^T(s)ds > \epsilon_0 I, \quad \forall t > 0,$$

with $I \in \mathcal{R}^{m\times m}$ being the identity matrix.

Analytically, the PE assumption implies that the subset $\{\Gamma(s); t \le s \le t+\tau\}$ spans the parameter space $\mathcal{R}^m$ for any $t$. Since $\Gamma(t)$ only relies on the known signals $\phi_1(t)$, $\phi_2(0,t)$, $\phi_3(t)$, $\phi_4(t)$ and auxiliary function $\Omega(\sigma)$, it is easy to get that the PE condition is satisfied if the frequency spectra of the known signals $\phi_1(t)$, $\phi_2(0,t)$, $\phi_3(t)$, $\phi_4(t)$ are rich enough.

Since $\det(Q(0)) \neq 0$, it follows from the equality $Q(t)Q^{-1}(t) = I$ that

$$\begin{aligned} 0 &= \frac{\mathrm{d}}{\mathrm{d}t}(I) = \frac{\mathrm{d}}{\mathrm{d}t}(Q(t)Q^{-1}(t)) \\ &= \frac{\mathrm{d}}{\mathrm{d}t}(Q(t))Q^{-1}(t) + Q(t)\frac{\mathrm{d}}{\mathrm{d}t}(Q^{-1}(t)), \end{aligned} \tag{23}$$

which means that

$$\frac{\mathrm{d}}{\mathrm{d}t}(Q(t)) = -Q(t)\frac{\mathrm{d}}{\mathrm{d}t}(Q^{-1}(t))Q(t). \tag{24}$$

Together with (21b), we get

$$\begin{aligned} \dot{Q}^{-1}(t) &= -Q^{-1}(t)\dot{Q}(t)Q^{-1}(t) \\ &= -\alpha Q^{-1}(t) + \Gamma(t)\Gamma^T(t). \end{aligned} \tag{25}$$

According to Ref. [25], we obtain that $Q^{-1}(t)$ is positive definite matrix and stays bounded away from 0 under the PE condition, which implies that one exists two constants $\epsilon_1, \epsilon_2$ satisfying $0 < \epsilon_1 < \epsilon_2$ such that

$$\epsilon_1 I \le Q^{-1}(t) \le \epsilon_2 I, \quad \forall t \ge 0. \tag{26}$$

Noticing that the parameter adaptive law (21a)–(21b) we established is very similar to the so-called forgetting-factor adaptive least-squares in Ref. [25]. The reader can refer to Reference [25] for more details about least-squares with forgetting factor and PE Assumption.

In particular, we rewrite the error system consisting of (11), (17), (20), (21a)–(21b) and (25) in the following form

$$\dot{Z}(t) = \left(A - LC\Omega^{-1}(\ell)\right)Z(t) - Lw(0,t), \tag{27a}$$

$$w_t(\sigma,t) = hw_{\sigma\sigma}(\sigma,t) + \tilde{g}(\sigma,t), \tag{27b}$$

$$w_\sigma(0,t) = 0, \tag{27c}$$

$$w(\ell,t) = 0, \tag{27d}$$

$$\begin{aligned} \dot{\tilde{\rho}}(t) = &-Q(t)\Gamma(t)\Gamma^T(t)\tilde{\rho}(t) \\ &-Q(t)\Gamma(t)\left(w(0,t) + C\Omega^{-1}(\ell)Z(t)\right), \end{aligned} \tag{27e}$$

$$\dot{Q}^{-1}(t) = -\alpha Q^{-1}(t) + \Gamma(t)\Gamma^T(t), \tag{27f}$$

where $\tilde{g}(\sigma,t) = g(\hat{u}(\sigma,t),\sigma,t) - g(u(\sigma,t),\sigma,t)$. For the sake of convenience, the complete adaptive observer structure is listed in Table 1.

*Remark 4* The well-posedness of the plant consisting of (2a)–(2d) and the observer system in Table 1 is analyzed in Appendix B. From [28, Theorem 3.3.3], we conclude that the inequality (3) is a sufficient condition to guarantee the existence and uniqueness of solution of the considered system.

*Remark 5* Compared with other types of observers, adaptive observers can estimate unknown states and parameters online. In this paper, only the boundary state $u(0,t)$ is available for measurement, we design an adaptive boundary observer based on the least-squares

**Table 1** Adaptive observer

*State observer*

$$\dot{\hat{X}}(t) = A\hat{X}(t) + \phi_1(t)\hat{\rho}_1(t) - L\big(\hat{u}(0,t) - u(0,t)\big) + \sum_{i=1}^{4} \lambda_{1i}(t)\dot{\hat{\rho}}_i(t),$$

$$\hat{u}_t(\sigma,t) = h\hat{u}_{\sigma\sigma}(\sigma,t) + g(\hat{u}(\sigma,t),\sigma,t) + \phi_2(\sigma,t)\hat{\rho}_2(t) - C\Omega(\sigma)\Omega^{-1}(\ell)L(\hat{u}(0,t) - u(0,t)) + \sum_{i=1}^{4}\big(\lambda_{2i}(\sigma,t) + C\Omega(\sigma)\Omega^{-1}(\ell)\lambda_{1i}(t)\big)\dot{\hat{\rho}}_i(t),$$

$$\hat{u}_\sigma(0,t) = \phi_3(t)\hat{\rho}_3(t),$$

$$\hat{u}(\ell,t) = C\hat{X}(t) + \phi_4(t)\hat{\rho}_4(t),$$

with $\lambda_{1i}(t) \in \mathcal{R}^{n\times m_i}$, $\lambda_{2i}(\sigma,t) \in \mathcal{R}^{1\times m_i}$ $(i = 1,2,3,4)$,

and $\Omega(\sigma) = \begin{pmatrix} I & 0 \end{pmatrix} e^{\begin{pmatrix} 0 & \frac{A}{h} \\ I & 0 \end{pmatrix}\sigma} \begin{pmatrix} I \\ 0 \end{pmatrix} \in \mathcal{R}^{n\times n}$.

*Filters*

$$\dot{\lambda}_{11}(t) = \big(A - LC\Omega^{-1}(\ell)\big)\lambda_{11}(t) + \phi_1(t) - L\lambda_{21}(0,t),$$

$$\dot{\lambda}_{12}(t) = \big(A - LC\Omega^{-1}(\ell)\big)\lambda_{12}(t) - L\lambda_{22}(0,t),$$

$$\dot{\lambda}_{13}(t) = \big(A - LC\Omega^{-1}(\ell)\big)\lambda_{13}(t) - L\lambda_{23}(0,t),$$

$$\dot{\lambda}_{14}(t) = \big(A - LC\Omega^{-1}(\ell)\big)\lambda_{14}(t) - L\lambda_{24}(0,t),$$

$$\lambda_{21,t}(\sigma,t) = h\lambda_{21,\sigma\sigma}(\sigma,t) - C\Omega(\sigma)\Omega^{-1}(\ell)\phi_1(t),$$

$$\lambda_{22,t}(\sigma,t) = h\lambda_{22,\sigma\sigma}(\sigma,t) + \phi_2(\sigma,t),$$

$$\lambda_{23,t}(\sigma,t) = h\lambda_{23,\sigma\sigma}(\sigma,t),$$

$$\lambda_{24,t}(\sigma,t) = h\lambda_{24,\sigma\sigma}(\sigma,t),$$

$$\lambda_{21,\sigma}(0,t) = 0, \quad \lambda_{22,\sigma}(0,t) = 0, \quad \lambda_{23,\sigma}(0,t) = \phi_3(t), \quad \lambda_{24,\sigma}(0,t) = 0,$$

$$\lambda_{21}(\ell,t) = 0, \quad \lambda_{22}(\ell,t) = 0, \quad \lambda_{23}(\ell,t) = 0, \quad \lambda_{24}(\ell,t) = \phi_4(t).$$

*Parameter estimator*

$$\dot{\hat{\rho}}(t) = -Q(t)\Gamma(t)\tilde{u}(0,t), \quad \dot{Q}(t) = \alpha Q(t) - Q(t)\Gamma(t)\Gamma^T(t)Q(t),$$

where $Q(t) \in \mathcal{R}^{m\times m}$, $Q(0) = Q_0 = Q_0^T > 0$,

and $\Gamma(t) = \begin{pmatrix} \big(C\Omega^{-1}(\ell)\lambda_{11}(t) + \lambda_{21}(0,t)\big)^T \\ \big(C\Omega^{-1}(\ell)\lambda_{12}(t) + \lambda_{22}(0,t)\big)^T \\ \big(C\Omega^{-1}(\ell)\lambda_{13}(t) + \lambda_{23}(0,t)\big)^T \\ \big(C\Omega^{-1}(\ell)\lambda_{14}(t) + \lambda_{24}(0,t)\big)^T \end{pmatrix} \in \mathcal{R}^m$ .

update law. Under an ad hoc persistent excitation condition, the estimation of unknown parameters and states can converge to the true value, thus eliminating the impact of uncertainty on the system performance.

## 4 Adaptive observer analysis

In this part, we plan to analyze stability of the error system consisting of (27a)–(27f). The main theoretical results will be given. First, we discuss the nonlinear function $\tilde{g}$ by means of the mean value theorem, which will be used in the stability analysis.

Utilizing the mean value theorem and the decoupling transformation (6a)–(6b), it follows that

$$\tilde{g}(\sigma,t) = \pi(\sigma,t)\Big(w(\sigma,t) + C\Omega(\sigma)\Omega^{-1}(\ell)Z(t) + \sum_{i=1}^{4} C\Omega(\sigma)\Omega^{-1}(\ell)\lambda_{1i}(t)\tilde{\rho}_i(t) + \sum_{i=1}^{4}\lambda_{2i}(\sigma,t)\tilde{\rho}_i(t)\Big), \tag{28}$$

with

$$\pi(\sigma,t) = \int_0^1 \frac{\partial g}{\partial u}(u(\sigma,t) + s\tilde{u}(\sigma,t),\sigma,t)ds. \tag{29}$$

Next, we give the boundedness of the auxiliary states $\lambda_{1i}(t)$ and $\lambda_{2i}(\sigma,t)(i=1,2,3,4)$ given by (10), (15) and (19).

**Lemma 1** *There has a real scalar $\lambda_M$ such that the auxiliary states $\lambda_{1i}(t)$ and $\lambda_{2i}(\sigma,t)(i=1,2,3,4)$ have the ensuing properties:*

$$\|\lambda_{1i}(t)\| \le \lambda_M, \quad \|\lambda_{2i}(\sigma,t)\| \le \lambda_M. \tag{30}$$

*Proof* In order to make the structure of the article clearer, the proof of the lemma is put in Appendix C. □

After, we establish the stability analysis of the observer system, which is also the most important result of this article.

**Theorem 1** *Consider the system (2a)–(2d) and the adaptive observer of Table 1 with the initial values $X(0)\in\mathcal{R}^n, u(\cdot,0)\in H^1(0,\ell)$ and the initial estimates $\hat{X}(0)\in\mathcal{R}^n, \hat{u}(\cdot,0)\in H^1(0,\ell)$ and $\hat{\rho}(0)\in\mathcal{R}^m$, choosing the appropriate constant $\alpha$, and suppose that Lemma 1 holds. If the diffusion coefficient $h$, the domain length $\ell$ and the coefficient $\beta$ meet $0<\beta\ell^2<\frac{\pi^2}{4}h$, then, the observer is globally exponentially convergent as $t\to\infty$, i.e., $\tilde{X}(t)$, $\tilde{u}(\sigma,t)$ and $\tilde{\rho}(t)$ converge exponentially to zero as $t\to\infty$.*

*Proof* In this part, the exponential stability of the plant (27a)–(27f) will be established. We discuss the ensuing Lyapunov–Krasovskii functional

$$\begin{aligned} V(t) &= Z^T(t)PZ(t)+\frac{a}{2}\int_0^\ell w^2(\sigma,t)d\sigma \\ &\quad+\frac{b}{2}\int_0^\ell w_\sigma^2(\sigma,t)d\sigma+\tilde{\rho}^T(t)Q^{-1}(t)\tilde{\rho}(t), \end{aligned} \tag{31}$$

where $a, b$ are positive scalars and $P$ is a positive definite symmetric matrix that meets the ensuing Lyapunov equation

$$P\big(A-LC\Omega^{-1}(\ell)\big)+\big(A-LC\Omega^{-1}(\ell)\big)^T P\le -\mu I, \tag{32}$$

with $\mu$ being a positive scalar to be determined later. Since $A-LC\Omega^{-1}(\ell)$ is a Hurwitz matrix, it can be easily checked that $P$ exists. Next, we divide Lyapunov functional $V(t)$ into three parts, denoted as

$$V_1(t)=Z^T(t)PZ(t), \tag{33a}$$

$$V_2(t)=\frac{a}{2}\int_0^\ell w^2(\sigma,t)d\sigma+\frac{b}{2}\int_0^\ell w_\sigma^2(\sigma,t)d\sigma, \tag{33b}$$

$$V_3(t)=\tilde{\rho}^T(t)Q^{-1}(t)\tilde{\rho}(t). \tag{33c}$$

*Part I.* Differentiating (33a) with respect to time, it follows from (27a) and (32) that

$$\begin{aligned} \dot{V}_1(t) &= Z^T(t)\big(A-LC\Omega^{-1}(\ell)\big)^T PZ(t) \\ &\quad+Z^T(t)P\big(A-LC\Omega^{-1}(\ell)\big)Z(t) \\ &\quad-2Z^T(t)PLw(0,t) \\ &\le -\mu\|Z(t)\|^2+\xi\|Z(t)\|^2+\frac{\|PL\|^2}{\xi}w^2(0,t) \\ &\le -(\mu-\xi)\|Z(t)\|^2+\frac{\ell\|PL\|^2}{\xi}\int_0^\ell w_\sigma^2(\sigma,t)d\sigma, \end{aligned} \tag{34}$$

with $\xi>0$ being a constant to be chosen later. In the last two steps, Young's inequality and (1b) are utilized, respectively.

*Part II.* Next, taking the time derivative of (33b) and utilizing (27b)–(27d), it follows that

$$\begin{aligned} \dot{V}_2(t) &= a\int_0^\ell w(\sigma,t)w_t(\sigma,t)d\sigma \\ &\quad+b\int_0^\ell w_\sigma(\sigma,t)w_{\sigma t}(\sigma,t)d\sigma \\ &= -ah\int_0^\ell w_\sigma^2(\sigma,t)d\sigma+a\int_0^\ell w(\sigma,t)\tilde{g}(\sigma,t)d\sigma \\ &\quad-b\int_0^\ell w_{\sigma\sigma}(\sigma,t)\big(hw_{\sigma\sigma}(\sigma,t)+\tilde{g}(\sigma,t)\big)d\sigma. \end{aligned} \tag{35}$$

Substituting (28) into (35) yields

$$\begin{aligned} \dot{V}_2(t) &= -ah\int_0^\ell w_\sigma^2(\sigma,t)d\sigma \\ &\quad+a\int_0^\ell w(\sigma,t)\pi(\sigma,t)w(\sigma,t)d\sigma \\ &\quad+a\int_0^\ell w(\sigma,t)\pi(\sigma,t)C\Omega(\sigma)\Omega^{-1}(\ell)Z(t)d\sigma \end{aligned}$$

$$
\begin{aligned}
&+a\int_0^\ell w(\sigma,t)\pi(\sigma,t)\\
&\sum_{i=1}^{4} C\Omega(\sigma)\Omega^{-1}(\ell)\lambda_{1i}(t)\tilde{\rho}_i(t)d\sigma\\
&+a\int_0^\ell w(\sigma,t)\pi(\sigma,t)\sum_{i=1}^{4}\lambda_{2i}(\sigma,t)\tilde{\rho}_i(t)d\sigma\\
&-bh\int_0^\ell w_{\sigma\sigma}^2(\sigma,t)d\sigma\\
&-b\int_0^\ell w_{\sigma\sigma}(\sigma,t)\pi(\sigma,t)w(\sigma,t)d\sigma\\
&-b\int_0^\ell w_{\sigma\sigma}(\sigma,t)\pi(\sigma,t)C\Omega(\sigma)\Omega^{-1}(\ell)Z(t)d\sigma\\
&-b\int_0^\ell w_{\sigma\sigma}(\sigma,t)\pi(\sigma,t)\\
&\sum_{i=1}^{4} C\Omega(\sigma)\Omega^{-1}(\ell)\lambda_{1i}(t)\tilde{\rho}_i(t)d\sigma\\
&-b\int_0^\ell w_{\sigma\sigma}(\sigma,t)\pi(\sigma,t)\sum_{i=1}^{4}\lambda_{2i}(\sigma,t)\tilde{\rho}_i(t)d\sigma.
\end{aligned}
\tag{36}
$$

For the second term of (36), by means of Young's inequality and together with (3), we get

$$
\left|a\int_0^\ell w(\sigma,t)\pi(\sigma,t)w(\sigma,t)d\sigma\right|\le a\beta\int_0^\ell w^2(\sigma,t)d\sigma. \tag{37}
$$

For the third term of (36), applying Young's inequality, we deduce

$$
\begin{aligned}
&a\int_0^\ell w(\sigma,t)\pi(\sigma,t)C\Omega(\sigma)\Omega^{-1}(\ell)Z(t)\mathrm{d}\sigma\\
&\le a\xi_1\|Z(t)\|^2\\
&+\frac{a}{4\xi_1}\int_0^\ell\|\pi(\sigma,t)C\Omega(\sigma)\Omega^{-1}(\ell)w(\sigma,t)\|^2\mathrm{d}\sigma\\
&\le a\xi_1\|Z(t)\|^2+\frac{a\delta\beta^2\ell}{4\xi_1}\int_0^\ell w^2(\sigma,t)\mathrm{d}\sigma,
\end{aligned}
\tag{38}
$$

where $\xi_1$ is an arbitrary scalar and $\delta\overset{\text{def}}{=}\sup_{\sigma\in[0,\ell]}\|C\Omega(\sigma)\Omega^{-1}(\ell)\|^2$. From the property $(a)$ in Appendix A, it can be easily checked that $\delta$ is bounded, due to function $\Omega(\sigma)$ is continuous on the closed interval $[0,\ell]$. Utilizing Young's inequality for the fourth term of (36), then recalling (3) and (29)–(30), we get

$$
\begin{aligned}
&a\int_0^\ell w(\sigma,t)\pi(\sigma,t)C\Omega(\sigma)\Omega^{-1}(\ell)\lambda_{11}(t)\tilde{\rho}_1(t)\mathrm{d}\sigma\\
&\le a\xi_2\|\tilde{\rho}_1(t)\|^2\\
&+\frac{a}{4\xi_2}\int_0^\ell\|\pi(\sigma,t)C\Omega(\sigma)\Omega^{-1}(\ell)\lambda_{11}(t)w(\sigma,t)\|^2\mathrm{d}\sigma\\
&\le a\xi_2\|\tilde{\rho}_1(t)\|^2+\frac{a\delta\lambda_M^2\beta^2\ell}{4\xi_2}\int_0^\ell w^2(\sigma,t)\mathrm{d}\sigma,
\end{aligned}
\tag{39}
$$

where $\xi_2>0$ is an arbitrary number. Thus, we obtain

$$
\begin{aligned}
&a\int_0^\ell w(\sigma,t)\pi(\sigma,t)\sum_{i=1}^{4}C\Omega(\sigma)\Omega^{-1}(\ell)\lambda_{1i}(t)\tilde{\rho}_i(t)\mathrm{d}\sigma\\
&\le a\xi_2\|\tilde{\rho}(t)\|^2+\frac{a\delta\lambda_M^2\beta^2\ell}{\xi_2}\int_0^\ell w^2(\sigma,t)\mathrm{d}\sigma.
\end{aligned}
\tag{40}
$$

By utilizing a similar approach to address the fifth term of (36), it follows that

$$
\begin{aligned}
&a\int_0^\ell w(\sigma,t)\pi(\sigma,t)\sum_{i=1}^{4}\lambda_{2i}(\sigma,t)\tilde{\rho}_i(t)\mathrm{d}\sigma\\
&\le a\xi_3\|\tilde{\rho}(t)\|^2+\frac{a\lambda_M^2\beta^2\ell}{\xi_3}\int_0^\ell w^2(\sigma,t)\mathrm{d}\sigma,
\end{aligned}
\tag{41}
$$

with $\xi_3>0$ being an arbitrary scalar. On the other hand, using Young's inequality for seventh term of (36) and integration by parts, then together with (3) and (29), we have

$$
\begin{aligned}
&b\int_0^\ell w_{\sigma\sigma}(\sigma,t)\pi(\sigma,t)w(\sigma,t)\mathrm{d}\sigma\\
&\le\frac{b\beta}{2\zeta_0}\int_0^\ell w^2(\sigma,t)d\sigma+\frac{b\beta\zeta_0}{2}\int_0^\ell w_{\sigma\sigma}^2(\sigma,t)\mathrm{d}\sigma,
\end{aligned}
\tag{42}
$$

where $\zeta_0>0$ is an arbitrary constant. Then, by means of Young's inequality for the eighth term of (36) yields

$$
\begin{aligned}
&b\int_0^\ell w_{\sigma\sigma}(\sigma,t)\pi(\sigma,t)C\Omega(\sigma)\Omega^{-1}(\ell)Z(t)\mathrm{d}\sigma\\
&\le b\zeta_1\|Z(t)\|^2\\
&+\frac{b}{4\zeta_1}\int_0^\ell\|\pi(\sigma,t)C\Omega(\sigma)\Omega^{-1}(\ell)w_{\sigma\sigma}(\sigma,t)\|^2\mathrm{d}\sigma\\
&\le b\zeta_1\|Z(t)\|^2+\frac{b\delta\beta^2\ell}{4\zeta_1}\int_0^\ell w_{\sigma\sigma}^2(\sigma,t)\mathrm{d}\sigma,
\end{aligned}
\tag{43}
$$

with $\zeta_1$ being an arbitrary scalar. Utilizing Young's inequality for the ninth term of (36), then together with (3) and (29)–(30), we have

$$\begin{aligned} & b\int_0^\ell w_{\sigma\sigma}(\sigma,t)\pi(\sigma,t)\sum_{i=1}^{4} \\ & C\Omega(\sigma)\Omega^{-1}(\ell)\lambda_{1i}(t)\tilde{\rho}_i(t)\mathrm{d}\sigma \\ \le & b\zeta_2\|\tilde{\rho}(t)\|^2+\frac{b\delta\lambda_M^2\beta^2\ell}{\zeta_2}\int_0^\ell w_{\sigma\sigma}^2(\sigma,t)\mathrm{d}\sigma, \end{aligned} \tag{44}$$

where $\zeta_2>0$ is an arbitrary scalar. By utilizing a similar approach to address the tenth term of (36), it follows that

$$\begin{aligned} & b\int_0^\ell w_{\sigma\sigma}(\sigma,t)\pi(\sigma,t)\sum_{i=1}^{4}\lambda_{2i}(\sigma,t)\tilde{\rho}_i(t)\mathrm{d}\sigma \\ \le & b\zeta_3\|\tilde{\rho}(t)\|^2+\frac{b\lambda_M^2\beta^2\ell}{\zeta_3}\int_0^\ell w_{\sigma\sigma}^2(\sigma,t\mathrm{d}\sigma, \end{aligned} \tag{45}$$

with $\zeta_3>0$ being an arbitrary scalar. Substituting (37)–(45) into (36) yields

$$\begin{aligned} \dot{V}_2(t)\le & -\Big\{ah-\frac{4\ell^2a\beta}{\pi^2}\Big(1+\frac{\delta\beta\ell}{4\xi_1}+\frac{\delta\lambda_M^2\beta\ell}{\xi_2}+\frac{\lambda_M^2\beta\ell}{\xi_3}\Big) \\ & -\frac{2\ell^2b\beta}{\pi^2\zeta_0}\Big\}\int_0^\ell w_\sigma^2(\sigma,t)\mathrm{d}\sigma \\ & -b\Big(h-\frac{\beta\zeta_0}{2}-\frac{\delta\beta^2\ell}{4\zeta_1}-\frac{\delta\lambda_M^2\beta^2\ell}{\zeta_2}-\frac{\delta\lambda_M^2\beta^2\ell}{\zeta_3}\Big) \\ & \int_0^\ell w_{\sigma\sigma}^2(\sigma,t)\mathrm{d}\sigma \\ & +\big(a\xi_2+a\xi_3+b\zeta_2+b\zeta_3\big)\|\tilde{\rho}(t)\|^2 \\ & +(a\xi_1+b\zeta_1)\|Z(t)\|^2. \end{aligned} \tag{46}$$

*Part III.* Differentiating (33c) with respect to $t$ and substituting (27e)–(27f), then utilizing Young's inequality, we deduce

$$\begin{aligned} \dot{V}_3(t) &= \tilde{\rho}^T(t)\dot{Q}^{-1}(t)\tilde{\rho}(t)+2\tilde{\rho}^T(t)Q^{-1}(t)\dot{\tilde{\rho}}(t) \\ &= \tilde{\rho}^T(t)\big(-\alpha Q^{-1}(t)+\Gamma(t)\Gamma^T(t)\big)\tilde{\rho}(t) \\ &\quad -2\tilde{\rho}^T(t)\Gamma(t)\big(\Gamma^T(t)\tilde{\rho}(t)+w(0,t) \\ &\quad +C\Omega^{-1}(\ell)Z(t)\big) \\ &\le -\alpha\tilde{\rho}^T(t)Q^{-1}(t)\tilde{\rho}(t)+8w^2(0,t) \\ &\quad +\frac{8}{7}\|C\Omega^{-1}(\ell)Z(t)\|^2. \end{aligned}$$

Together with (26) and Wirtinger's inequality (1b), one has

$$\begin{aligned} \dot{V}_3(t) \le & -\alpha\epsilon_1\|\tilde{\rho}(t)\|^2+8\ell\int_0^\ell w_\sigma^2(\sigma,t)d\sigma \\ & +\frac{8}{7}\delta_1\|Z(t)\|^2, \end{aligned} \tag{47}$$

where $\delta_1\overset{\text{def}}{=}\|C\Omega^{-1}(\ell)\|^2<\infty$.

Then, adding (34) and (46)–(47) together, we get

$$\begin{aligned} \dot{V}(t)\le & -\Big\{ah-\frac{4\ell^2a\beta}{\pi^2}\Big(1+\frac{\delta\beta\ell}{4\xi_1}+\frac{\delta\lambda_M^2\beta\ell}{\xi_2}+\frac{\lambda_M^2\beta\ell}{\xi_3}\Big) \\ & -\frac{2\ell^2b\beta}{\pi^2\zeta_0}-\frac{\ell\|PL\|^2}{\xi}-8\ell\Big\}\int_0^\ell w_\sigma^2(\sigma,t)d\sigma \\ & -b\Big(h-\frac{\beta\zeta_0}{2}-\frac{\delta\beta^2\ell}{4\zeta_1}-\frac{\delta\lambda_M^2\beta^2\ell}{\zeta_2}-\frac{\delta\lambda_M^2\beta^2\ell}{\zeta_3}\Big) \\ & \int_0^\ell w_{\sigma\sigma}^2(\sigma,t)d\sigma \\ & -(\mu-\xi-a\xi_1-b\zeta_1-\frac{8}{7}\delta_1)\|Z(t)\|^2 \\ & -\big(\alpha\epsilon_1-a\xi_2-a\xi_3-b\zeta_2-b\zeta_3\big)\|\tilde{\rho}(t)\|^2. \end{aligned} \tag{48}$$

Then, we choose the free coefficient $\zeta_0=\frac{h}{\beta}$ and assume that the diffusion coefficient $h$, the domain length $\ell$, the coefficient $\beta$ and other (free) positive numbers $(\mu,a,b,\alpha,\xi,\xi_1,\xi_2,\xi_3,\zeta_1,\zeta_2,\zeta_3)$ satisfy the following inequalities:

$$\begin{aligned} & ah-\frac{4\ell^2a\beta}{\pi^2}\Big(1+\frac{\delta\beta\ell}{4\xi_1}+\frac{\delta\lambda_M^2\beta\ell}{\xi_2}+\frac{\lambda_M^2\beta\ell}{\xi_3}\Big) \\ & -\frac{2\ell^2b\beta^2}{\pi^2h}-\frac{\ell\|PL\|^2}{\xi}-8\ell>\epsilon a>0, \end{aligned} \tag{49a}$$

$$\frac{h}{2}-\frac{\delta\beta^2\ell}{4\zeta_1}-\frac{\delta\lambda_M^2\beta^2\ell}{\zeta_2}-\frac{\delta\lambda_M^2\beta^2\ell}{\zeta_3}>\frac{h}{4}>0, \tag{49b}$$

$$\mu-\xi-a\xi_1-b\zeta_1-\frac{8}{7}\delta_1>\frac{\mu-\xi}{2}>0, \tag{49c}$$

$$\alpha\epsilon_1-a\xi_2-a\xi_3-b\zeta_2-b\zeta_3>\frac{\alpha\epsilon_1}{2}>0, \tag{49d}$$

for certain $0<\epsilon<1$. For simplicity, we define

**Fig. 2** Maximal admissible Lipschitz coefficient $\beta$ for different $\ell$ when the diffusion coefficient $h$ is fixed

| $h$ | 1 | 1 | 1 | 1 | 1 | 2 | 2 | 2 | 2 | 2 |
|---|---|---|---|---|---|---|---|---|---|---|
| $l$ | 0.5 | 1 | 2 | 3 | 4 | 0.5 | 1 | 2 | 3 | 4 |
| $\beta$ | 9.8696 | 2.4674 | 0.6169 | 0.2742 | 0.1542 | 19.7392 | 4.9348 | 1.2337 | 0.5483 | 0.3084 |

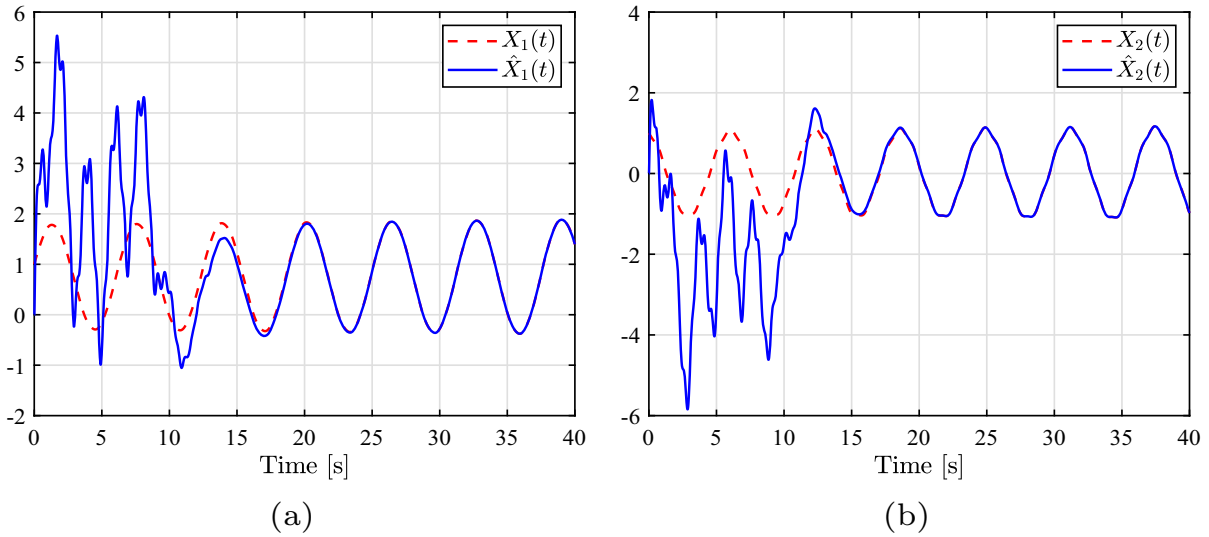


**Fig. 3** The trajectories of the ODE state $X(t)$ and its estimate $\hat{X}(t)$ in Example 1. **a** $X_1(t)$ and its estimate $\hat{X}_1(t)$; **b** $X_2(t)$ and its estimate $\hat{X}_2(t)$

$$\chi_1 = \frac{\pi^2}{2a\ell^2}\Big\{ah - \frac{4\ell^2 a\beta}{\pi^2}\Big(1 + \frac{\delta\beta\ell}{4\xi_1} + \frac{\delta\lambda_M^2\beta\ell}{\xi_2} + \frac{\lambda_M^2\beta\ell}{\xi_3}\Big) - \frac{2\ell^2 b\beta}{\zeta_0\pi^2} - \frac{\ell\|PL\|^2}{\xi} - 8\ell\Big\},$$

$$\chi_2 = \frac{\pi^2}{2\ell^2}\Big(h - \frac{\beta\zeta_0}{2} - \frac{\delta\beta^2\ell}{4\zeta_1} - \frac{\delta\lambda_M^2\beta^2\ell}{\zeta_2} - \frac{\delta\lambda_M^2\beta^2\ell}{\zeta_3}\Big),$$

$$\chi_3 = \big(\mu - \xi - a\xi_1 - b\zeta_1 - \frac{8}{7}\delta_1\big)\frac{1}{\lambda_{\min}(P)},$$

$$\chi_4 = \alpha - (a\xi_2 + a\xi_3 + b\zeta_2 + b\zeta_3)\frac{1}{\epsilon_1}.$$

By means of (49a)–(49d), it follows that

$$\chi(\ell) =: \min\Big\{\frac{\epsilon\pi^2}{2\ell^2}, \frac{\pi^2 h}{8\ell^2}, \frac{\mu-\xi}{2\lambda_{\min}(P)}, \frac{\alpha}{2}\Big\} \le \min\{\chi_1, \chi_2, \chi_3, \chi_4\}.$$

Together with (31), (48) and (49a)–(49d), we get

$$\dot{V}(t) \le -\chi(\ell)V(t),$$

which means that $V(t)$ is exponentially vanishing as $t \to \infty$. From (31), we can easily verify that $Z(t)$, $\tilde{\rho}(t)$, $\int_0^\ell w^2(\sigma,t)d\sigma$ and $\int_0^\ell w_\sigma^2(\sigma,t)d\sigma$ are exponentially vanishing as $t \to \infty$. Together with Wirtinger's inequality (1b), so is $w(\sigma,t)$.

Furthermore, due to $\lambda_{1i}(t)$ and $\lambda_{2i}(\sigma,t)$ $(i = 1,2,3,4)$ and $\Omega(\sigma)$ are bounded, $Z(t)$, $\tilde{\rho}(t)$ and $w(\sigma,t)$ are exponentially vanishing as $t \to \infty$, so are $\tilde{X}(t)$ and $\tilde{u}(\sigma,t)$ by the decoupling transformation (6a)–(6b).

Finally, we verify the above conditions (49a)–(49d) hold. Owing to (49a), it holds if the ensuing couple of inequalities do so:

$$h - \frac{4\ell^2\beta}{\pi^2} - \frac{\delta\ell^3\beta^2}{\xi_1\pi^2} - \frac{4\ell^3\delta\lambda_M^2\beta^2}{\xi_2\pi^2} - \frac{4\ell^3\lambda_M^2\beta^2}{\xi_3\pi^2} > \frac{\epsilon}{2}, \tag{50a}$$

$$\frac{2\ell^2 b\beta}{\pi^2 h} + \frac{\ell\|PL\|^2}{\xi} + 8\ell < a\frac{\epsilon}{2}. \tag{50b}$$

Due to $0 < \epsilon < 1$ is free and in Theorem 1, it is supposed that $\frac{4\beta\ell^2}{\pi^2} < h$. Taking $\epsilon = h - \frac{4\beta\ell^2}{\pi^2}$, it is

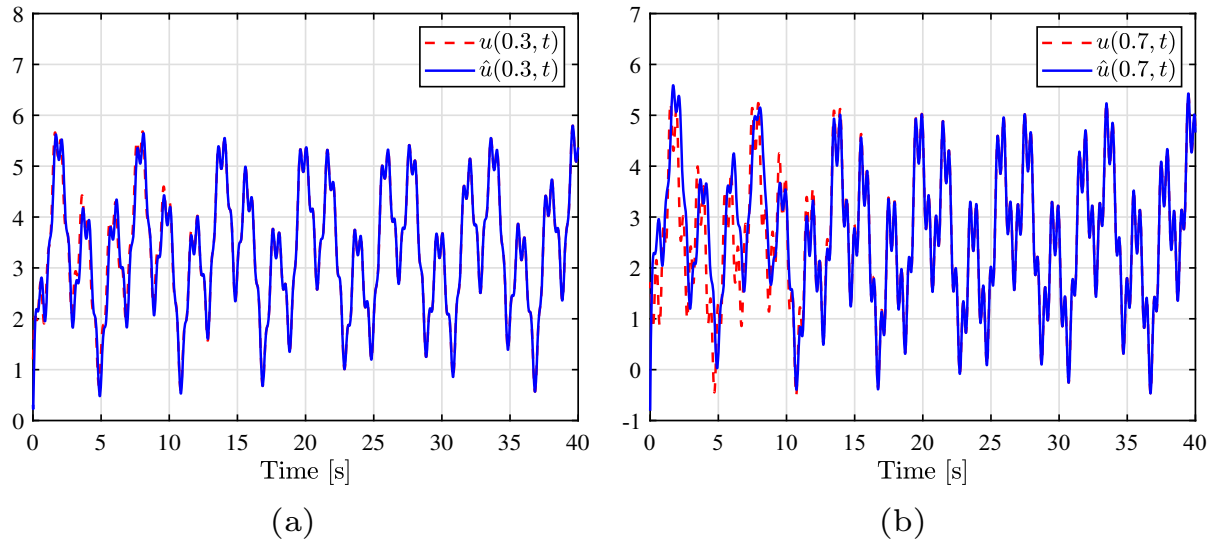


**Fig. 4** The trajectories of the PDE state $u(\sigma, t)$ and the observer state $\hat{u}(\sigma, t)$ when $\sigma = 0.3$ and $\sigma = 0.7$ in Example 1

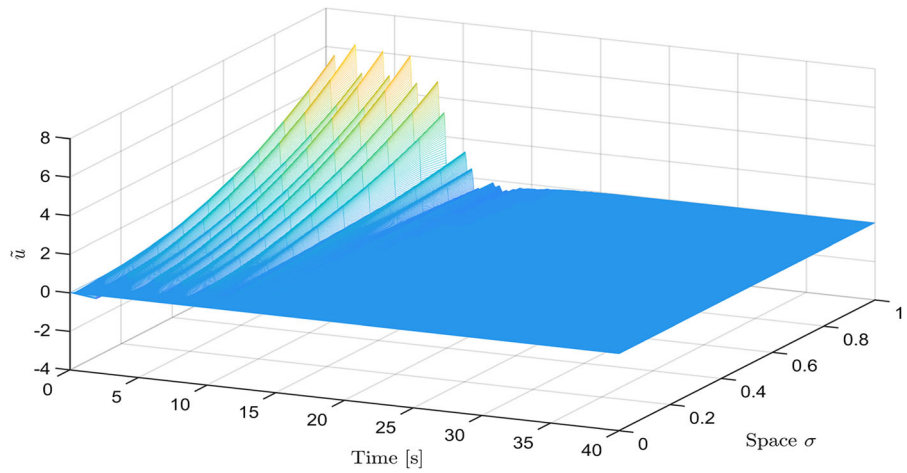


**Fig. 5** The trajectory of the PDE state estimation error $\tilde{u}(\sigma, t) = \hat{u}(\sigma, t) - u(\sigma, t)$ in Example 1

easy to check that (50a) holds if $\xi_i (i = 1, 2, 3)$ satisfy

$$\xi_1 > \frac{8\delta\ell^3\beta^2}{h\pi^2 - 4\ell^2\beta}, \quad \xi_2 > \frac{32\delta\ell^3\lambda_M^2\beta^2}{h\pi^2 - 4\ell^2\beta}, \quad \xi_3 > \frac{32\ell^3\lambda_M^2\beta^2}{h\pi^2 - 4\ell^2\beta}, \tag{51}$$

In addition, we take $a$ sufficiently large and an appropriate $\xi$ such that $b$ satisfies

$$0 < b < \frac{a\xi h(h\pi^2 - 4\ell^2\beta) - 16\xi\ell h\pi^2 - 2\ell h\pi^2\|PL\|^2}{4\xi\ell^2\beta}, \tag{52}$$

which implies that (50b) holds. Thus, we infer that (49a) holds. Then, taking

$$\zeta_1 > \frac{3\delta\beta^2\ell}{h}, \quad \zeta_2 > \frac{12\delta\lambda_M^2\beta^2\ell}{h}, \quad \zeta_3 > \frac{12\delta\lambda_M^2\beta^2\ell}{h}, \tag{53}$$

it is easy to give that (49b) holds. In addition, we select

$$\mu > \xi + a\xi_1 + b\zeta_1 + \frac{8}{7}\delta_1, \quad \alpha > \frac{a\xi_2 + a\xi_3 + b\zeta_2 + b\zeta_3}{\epsilon_1}, \tag{54}$$

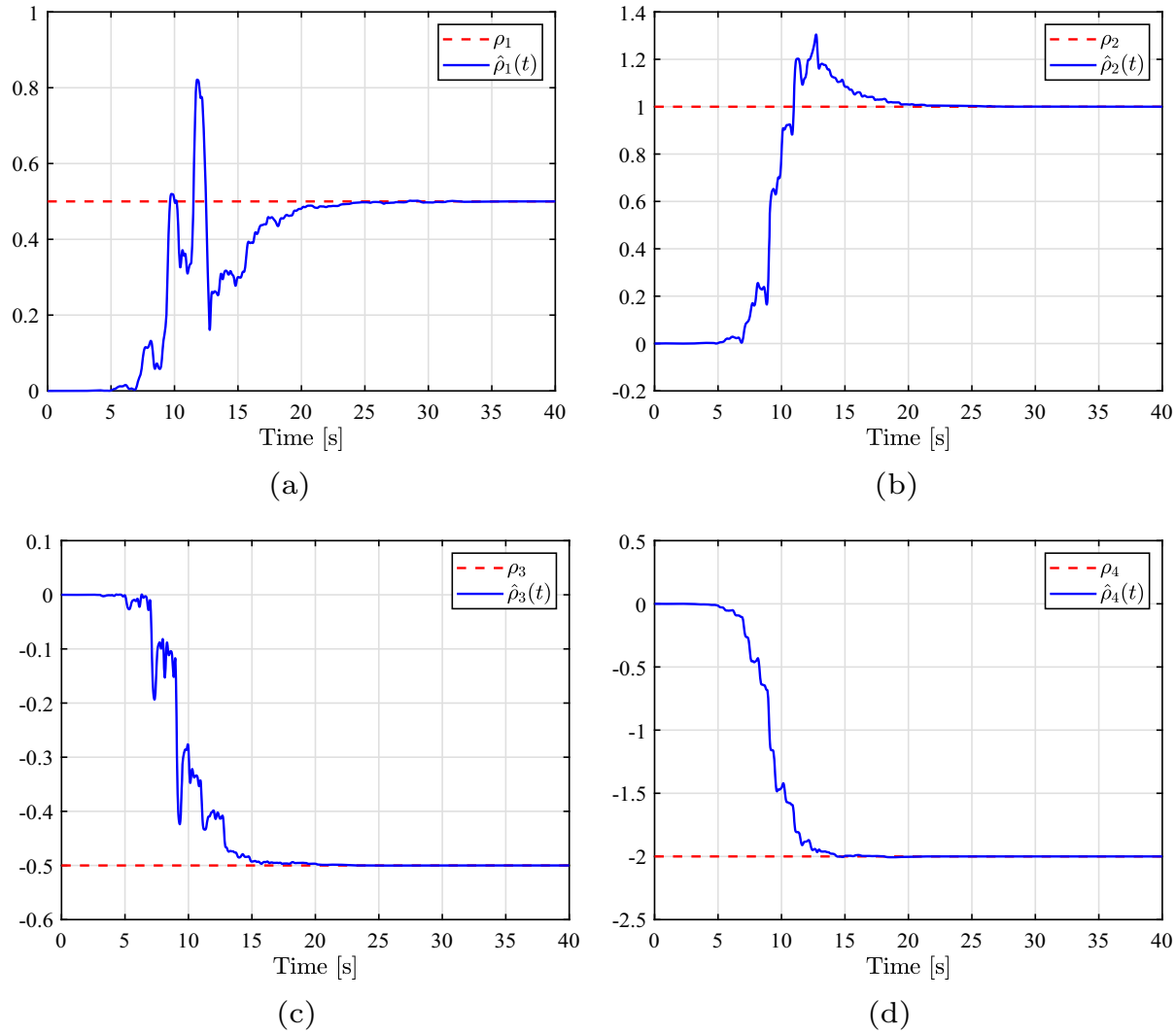


**Fig. 6** The trajectories of the fixed system parameters $\rho_i (i = 1, 2, 3, 4)$ and their estimate values $\hat{\rho}_i(t)$ in Example 1. **a** $\rho_1(t)$ and $\hat{\rho}_1(t)$; **b** $\rho_2(t)$ and $\hat{\rho}_2(t)$; **c** $\rho_3(t)$ and $\hat{\rho}_3(t)$; **d** $\rho_4(t)$ and $\hat{\rho}_4(t)$

we get (49c)–(49d) hold. In general, inequalities (49a)–(49d) can be easily verified by selecting appropriate free parameters $(\mu, a, b, \alpha, \xi, \xi_1, \xi_2, \xi_3, \zeta_1, \zeta_2, \zeta_3)$ provided that $\frac{4\beta\ell^2}{\pi^2} < h$.

In this way, the result of Theorem 1 is given. □

*Remark 6* (i) From the condition $0 < \beta\ell^2 < \frac{\pi^2}{4}h$ of Theorem 1, we can see that once $h$ is fixed, there is a dependence between the domain length $\ell$ and the coefficient $\beta$, neither of which can be arbitrarily large. If the region length $\ell$ is large, then the coefficient $\beta$ is small and vice versa. Moreover, if $\beta = 0$, then the condition $0 < \beta\ell^2 < \frac{\pi^2}{4}h$ is satisfied for all $\ell$, which also indicates that Ref. [20] is the special case of this paper.

(ii) In Theorem 1, we assume that the diffusion coefficient $h$, the domain length $\ell$ and the coefficient $\beta$ meet the condition $0 < \beta\ell^2 < \frac{\pi^2}{4}h$. As $h$ increases, the range of $\beta$ and $\ell$ increases. In a sense, we relax the condition of Reference [12, Theorem 1], because [12] is the special case of this paper when $h = 1$.

(iii) In the situation of arbitrary large coefficients $\beta$ and $\ell$, the current observer design can still be advantageous. Just as in the literature [23], as long as one places $M$ sensors along the domain. Then, by increas-

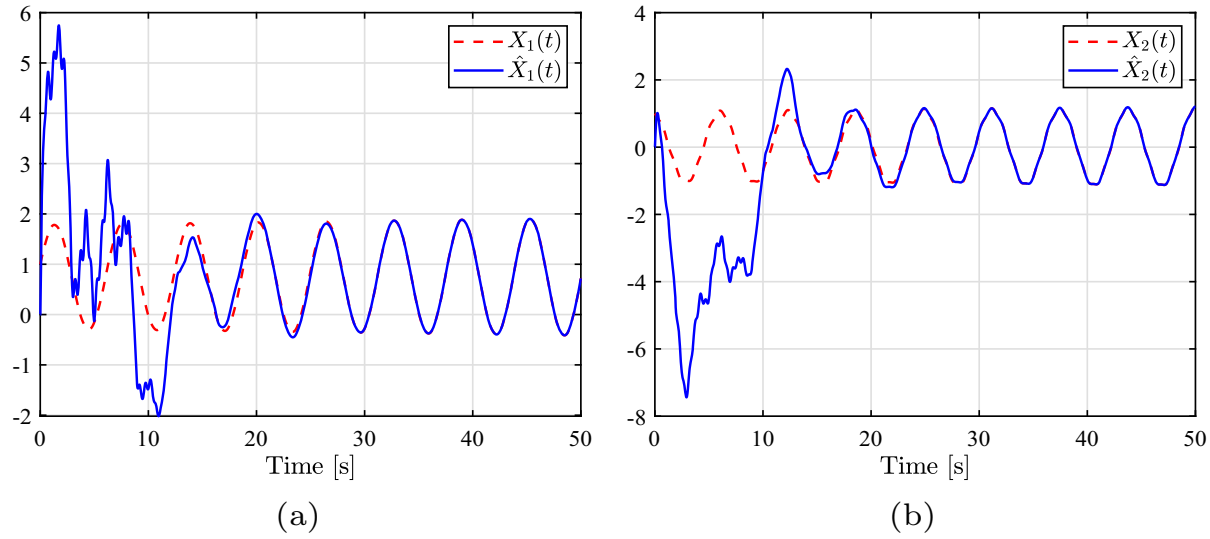


**Fig. 7** The trajectories of the ODE state $X(t)$ and its estimate $\hat{X}(t)$ in Example 2. **a** $X_1(t)$ and its estimate $\hat{X}_1(t)$; **b** $X_2(t)$ and its estimate $\hat{X}_2(t)$

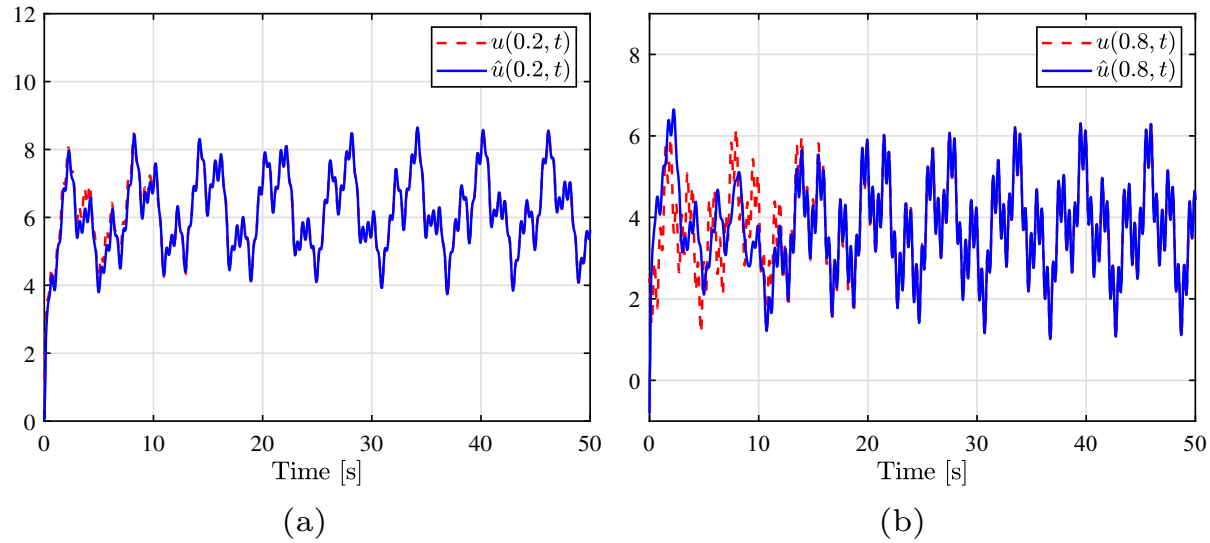


**Fig. 8** The trajectories of the PDE state $u(\sigma,t)$ and the observer state $\hat{u}(\sigma,t)$ when $\sigma = 0.3$ and $\sigma = 0.7$ in Example 2

ing the number $M$ of sensors, $\frac{\ell}{M}$ will be enough small, which can always be achieved.

*Remark 7* In practice, the inequality (32) is equivalently expressed by the bilinear matrix inequality (BMI): $PA - PLC\Omega^{-1}(\ell) + A^T P - (\Omega^{-1}(\ell))^T C^T L^T P < 0$. Letting $\Theta = PL$, then it is reduced to the linear matrix inequality (LMI):

$$PA - \Theta C\Omega^{-1}(\ell) + A^T P - (\Omega^{-1}(\ell))^T C^T \Theta < 0, \tag{55}$$

which can be solved by utilizing the MATLAB LMI toolbox. As stated in [6,7], if the value of the gain $L$ is known, then the LMI (55) holds true. Suppose if the value of the gain $L$ is unknown, then the LMI (55) turns to be nonlinear. To make it as linear one and to obtain an explicit solution of LMI, we can take any matrix $\Theta = PL$ in (55) and the gain can be solved by $L = P^{-1}\Theta$, such that $(A - LC\Omega^{-1}(\ell))$ is Hurwitz.

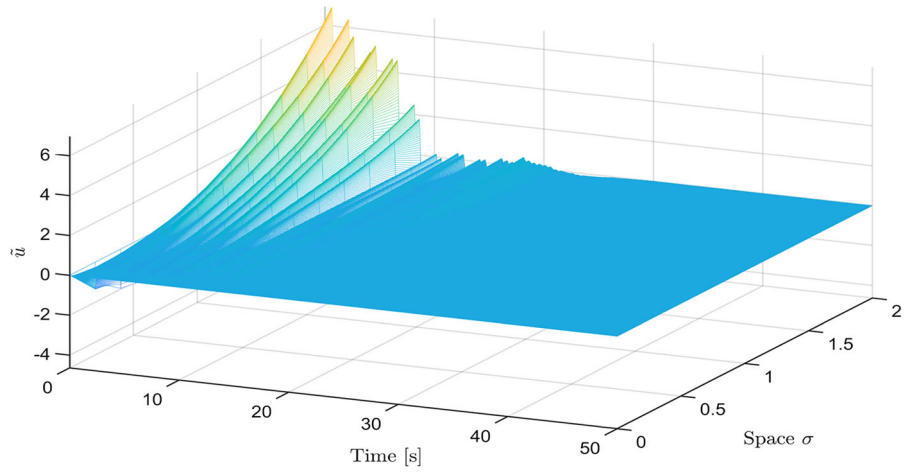


**Fig. 9** The trajectory of the PDE state estimation error $\tilde{u}(\sigma,t)=\hat{u}(\sigma,t)-u(\sigma,t)$ in Example 2

*Remark 8* The idea of taking the Lyapunov function $V_3(t)$ mainly depends on the structure of the least-square adaptive update law (21a)–(21b). First, according to (25) and the PE condition, $Q^{-1}(t)$ is a positive definite symmetric matrix, which meets the condition for designing Lyapunov function based on positive definite quadratic. Second, the use of $Q^{-1}(t)$ in $V_3(t)$ can skillfully deal with the term $Q(t)$ in the adaptive law (21a). The construction method of $V_3(t)$ is mainly derived from the literature [29], and readers can refer to [29] for more details.

## 5 Simulation analysis

In this part, we take the simplified catalytic reaction in a chemical reactor as a concrete example to verify the availability of the observer built in Table 1, where the PDE state $u(\sigma,t)\in\mathcal{R}$ denotes the temperature of a solid body, the term $g$ is the density of a heat resource generated by a chemical reaction. The ODE state $X(t)\in\mathcal{R}^n$ denotes the temperature of a fluid. The uncertainty terms $\phi_1(t)\rho_1,\phi_2(\sigma,t)\rho_2,\phi_3(t)\rho_3,\phi_4(t)\rho_4$ represent the interference of external factors to the system in practical application, including the particle size of the reactants, friction, contact area between the reactants, etc.

However, in practical applications, the method in this paper also has some limitations. When the diffusion coefficient $h$ is fixed, the domain length $\ell$ and Lipschitz coefficient $\beta$ cannot be arbitrarily large. As noted in Remark 6 (iii), multiple sensors are required if $\ell$ and $\beta$ are arbitrarily large, which increases the economic cost to some extent. The admissible condition between $\ell$ and $\beta$ is shown in Fig. 2. Next, we take two groups of parameters in the green part in Fig. 2 for verification in MATLAB software. Here, the forward Time Central Space (FTCS) finite difference method in Reference [30] is utilized to discretize time and space.

*Example 1* We consider the system (2a)–(2d) with the following parameters and functions: $A=\begin{bmatrix}0&1\\-1&0\end{bmatrix}$, $C=\begin{bmatrix}1,&0\end{bmatrix}$, $\phi_1(t)=\begin{bmatrix}0\\1+(\sin(3t))^2\end{bmatrix}$, $\phi_2(\sigma,t)=e^{0.2\sigma}(5+(\sin(3t))^2)$, $\phi_3(t)=\sin(4\pi t)+\sin(2\pi t)$, $\phi_4(t)=\sin(4\pi t)+\sin(\pi t)$, $g(u(\sigma,t),\sigma,t)=\beta\sin(u(\sigma,t))$, $h=1$, $\ell=1$, with the initial values $X_1(0)=X_2(0)=1$, $u(\sigma,0)=\sigma+1$. The system parameters $\rho_1=0.5$, $\rho_2=1$, $\rho_3=-0.5$ and $\rho_4=-2$ are assumed to be unknown. The observer established in Table 1 is considered with initial data $\hat{X}_1(0)=\hat{X}_2(0)=0$, $\hat{u}(\sigma,0)=\cos(2\pi\sigma)$, $\lambda_{1i}(0)=1(i=1,2,3,4)$, $\lambda_{2i}(\sigma,0)=0(i=1,2,3,4)$, $\hat{\rho}_1(0)=\hat{\rho}_2(0)=\hat{\rho}_3(0)=\hat{\rho}_4(0)=0$, $Q(0)=0.001I$.

The other parameters are selected as: $\beta=0.0617<2.4674$, $L=[16.8,\ 16.1]^T$, it can be obtained that $A-LC\Omega^{-1}(\ell)=\begin{bmatrix}-13.7957&8.1776\\-14.2208&6.8785\end{bmatrix}$. Next, let us verify the conditions (49a)–(49d). After a complicated calculation, taking $\xi_1=0.0032$, $\xi_2=\xi_3=0.1139$, $\zeta_1=0.0114$, $\zeta_2=\zeta_3=0.4109$, $\epsilon_1=42$, $P=\begin{bmatrix}1.8236&-1.6991\\-1.6991&1.8751\end{bmatrix}$, $\xi=\frac{\|PL\|^2}{30}$, $a=78$, $b=0.1$, it can be verified that the conditions (51)–(53) hold. Then, we can obtain that the eigenvalues

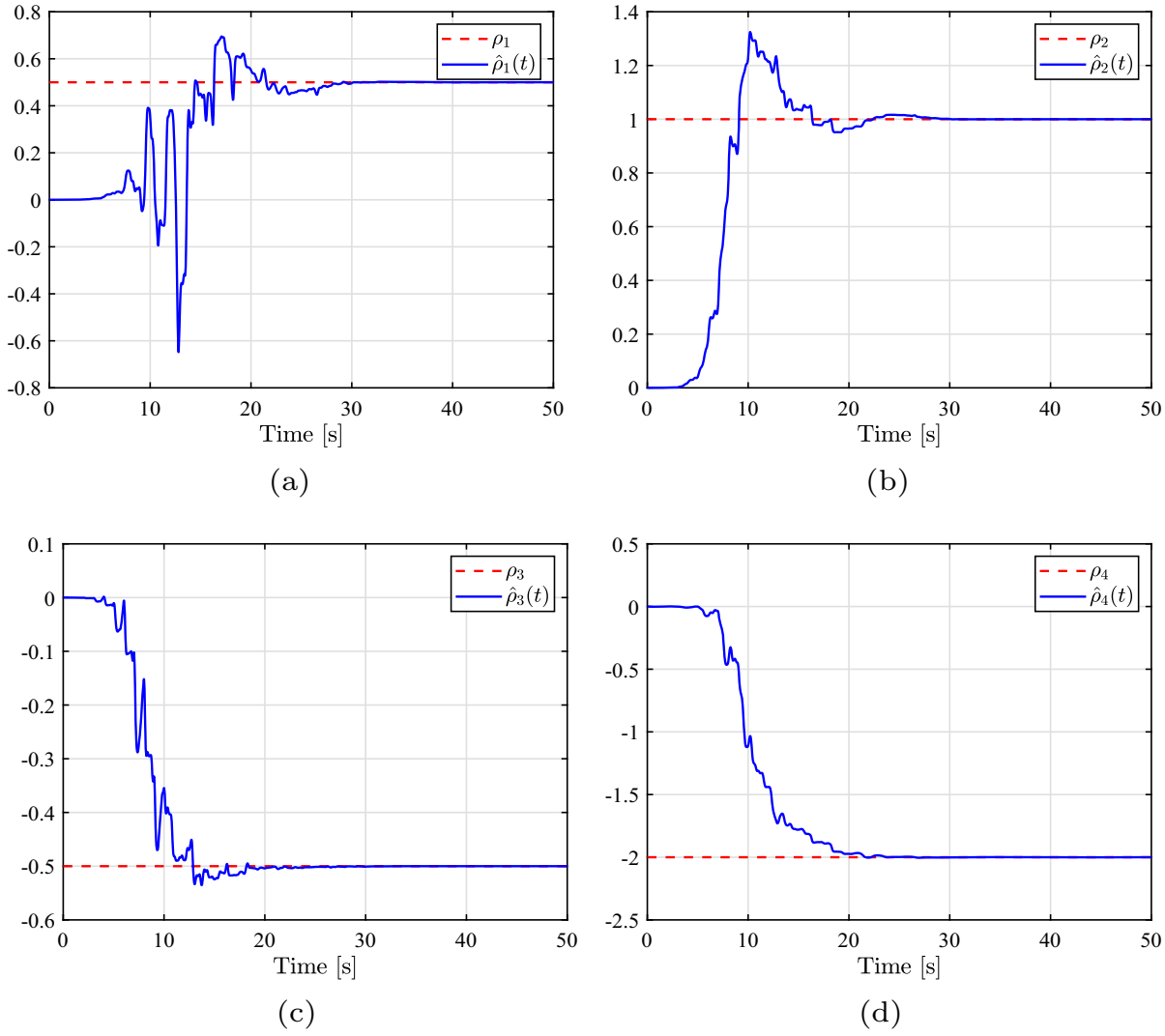


**Fig. 10** The trajectories of the fixed system parameters $\rho_i (i = 1, 2, 3, 4)$ and their estimate values $\hat{\rho}_i(t)$ in Example 2. **a** $\rho_1(t)$ and $\hat{\rho}_1(t)$; **b** $\rho_2(t)$ and $\hat{\rho}_2(t)$; **c** $\rho_3(t)$ and $\hat{\rho}_3(t)$; **d** $\rho_4(t)$ and $\hat{\rho}_4(t)$

of $(A - LC\Omega^{-1}(\ell))^T P + P(A - LC\Omega^{-1}(\ell))$ are $\{-1.9933, -1.9903\}$. Further, it follows from (54) that $\mu > 1.679$ and $\alpha > 0.43$. Thus, we take the design parameters $\alpha = 1.2$ and $\mu = 1.8$.

The simulation results of the system and observer are obtained and presented in Figs. 3, 4, 5, and 6. Figure 3 indicates that the estimate values $\hat{X}_1(t)$ and $\hat{X}_2(t)$ converge to the true values $X_1(t)$ and $X_2(t)$ after 15 s. Figure 4 gives the trajectories of the PDE state $u(\sigma, t)$ and its estimate $\hat{u}(\sigma, t)$ at two specified locations in the domain, i.e., $\sigma = 0.3$ and $\sigma = 0.7$. We can observe that after 15 s, the estimates $\hat{u}(0.3, t)$ and $\hat{u}(0.7, t)$ converge to the true values $u(0.3, t)$ and $u(0.7, t)$. Figure 5 illustrates that the evolution of the PDE state estimation error $\tilde{u}(\sigma, t)$. We can see that after 15 s, the error $\tilde{u}(\sigma, t)$ converges to zero. From Fig. 6, it can be observed that after a transient period of 15 s, parameter estimates $\hat{\rho}_i (i = 1, 2, 3, 4)$ are very close to their true values $\rho_i$. In summary, the simulation results Figs. 3, 4, 5, and 6 are conformity with the theoretical results.

*Example 2* Next, we will illustrate that the value range of the domain length $\ell$ and the Lipschitz coefficient $\beta$ increase with the increase of the diffusion coefficient $h$.

We consider the system (2a)–(2d) with the diffusion coefficient $h = 2$ and the domain length $\ell = 2$. The Lipschitz coefficient is selected as $\beta = 1.2337$. The gain $L = [12.8, 6.1]$ and the coefficient $\alpha = 1.2$, the other system parameters and initial data are the same as Example 1.

The simulation results of the system and observer are obtained and presented in Figs. 7, 8, 9, and 10. Figure 7 indicates that the estimate values $\hat{X}_1(t)$ and $\hat{X}_2(t)$ converge to the true values $X_1(t)$ and $X_2(t)$ after 20 s. Figure 8 gives the trajectories of the PDE state $u(\sigma, t)$ and its estimate $\hat{u}(\sigma, t)$ at two specified locations in the domain, i.e., $\sigma = 0.2$ and $\sigma = 0.8$. We can observe that after 20 s, the estimates $\hat{u}(0.2, t)$ and $\hat{u}(0.8, t)$ converge to the true values $u(0.2, t)$ and $u(0.8, t)$. Figure 9 illustrates that the evolution of the PDE state estimation error $\tilde{u}(\sigma, t)$. We can see that after 20 s, the error $\tilde{u}(\sigma, t)$ converges to zero. From Fig. 10, it can be observed that after a transient period of 20 s, parameter estimates $\hat{\rho}_i(t)(i = 1, 2, 3, 4)$ are very close to their true values $\rho_i$. In summary, the simulation results Figs. 7, 8, 9, and 10 are also conformity with the theoretical results.

## 6 Conclusion

In this article, we design an adaptive observer for ODE-PDE coupled systems subject to nonlinear dynamics and uncertain parameters through the decoupling transformation. The observer in Table 1 consists of the following four parts: (a) a state observer, which is a replicate of the system; (b) the matrix function $\Omega(\sigma)$; (c) auxiliary filters given by ODEs and PDEs; and (d) a least-squares parameter adaptive law. Finally, the exponentially vanishing of the adaptive observer is established by constructing a suitable Lyapunov–Krasovskii functional. However, the system output is not continuously measurable in many applications. How to design a sample-value adaptive observer for ODE-PDE cascade systems subject to nonlinear dynamics and parameter uncertainty is our next work. In addition, how to extend the research results of this paper to the parabolic PDE with uncertain nonlinear semi-Markov jumping signals in the literature [31] is also worthy of further study.

**Acknowledgements** This work was supported by the Shandong Provincial Natural Science Foundation (Grant No. ZR2021ZD13), the Taishan Scholarship Project of Shandong Province, and the National Natural Science Foundation of China (Grant No. 61873330).

**Data Availability Statement** The datasets analyzed during the current study are available from the corresponding author on reasonable.

**Declarations**

**Conflict the interest** The authors declare no conflict of interest in preparing this article.

**Human and animals rights** No human or animal subjects were used in this work.

## Appendix A: Properties of the matrix function $\Omega(\sigma)$

To the best of our knowledge, the matrix function $\Omega(\sigma)$ meets the ensuing properties:

$$(a)\quad \Omega(\sigma) = I + \sum_{k=1}^{n-1} \frac{\sigma^{2k}}{(2k)!}\left(\frac{A}{h}\right)^k,$$

$$(b)\quad A\Omega(\sigma) = \Omega(\sigma)A,$$

$$(c)\quad A\Omega^{-1}(\sigma) = \Omega^{-1}(\sigma)A,$$

$$(d)\quad \Omega(\sigma) \overset{\text{def}}{=} \begin{pmatrix} I & 0 \end{pmatrix} e^{\begin{pmatrix} 0 & \frac{A}{h} \\ I & 0 \end{pmatrix}\sigma} \begin{pmatrix} I \\ 0 \end{pmatrix}, \quad \forall \sigma \in \mathcal{R}.$$

The reader can refer to Ref. [9] for more details.

## Appendix B: The well-posedness of system

*Step 1.* We first show the well-posedness of the ODE-subsystem (2a) with the initial data $X(0)$. By utilizing the existence theorem of ODEs, the subsystem (2a) exists a unique solution $X(t) \in \mathcal{C}^1([0, +\infty) : \mathcal{R}^n)$.

*Step 2.* The well-posedness of the PDE-subsystem (2b)-(2d) will be illustrated. First, introducing the ensuing transformation for any $(\sigma, t) \in [0, \ell] \times [0, +\infty)$

$$q(\sigma, t) = u(\sigma, t) - C\Omega(\sigma)\Omega^{-1}(\ell)X(t). \tag{B.1}$$

Together with Appendix A, we rewrite the system (2b)–(2d) as

$$\begin{cases} q_t(\sigma, t) = hq_{\sigma\sigma}(\sigma, t) + \bar{g}(q, \sigma, t), \\ q_\sigma(0, t) = \phi_3(t)\rho_3, \\ q(\ell, t) = \phi_4(t)\rho_4, \end{cases}$$

where $\bar{g}(q, \sigma, t) = g(q + C\Omega(\sigma)\Omega^{-1}(\ell)X, \sigma, t) + \phi_2(\sigma, t)\rho_2 - C\Omega(\sigma)\Omega^{-1}(\ell)\phi_1(t)\rho_1$. Obviously, function $\bar{g}(\cdot)$ inherits all the properties of function $g(\cdot)$. The

$q$-subsystem turns out to be a special case of the semi-linear parabolic system (13)–(14) in Ref. [26]. It can be obtained that one has a strong solution $q(\sigma,t) \in \mathcal{H}^1(0,\ell)$ for each $t \geq 0$. Due to the fact that the transformation (B.1) is inverse, the similar result holds for PDE subsystem (2b)–(2d).

**Step 3.** In this part, we illustrate the well-posedness of the observer system of Table 1.

First, we develop the well-posedness of the error system (27a)–(27f). Applying the usual existence theorems for ODEs, it follows that the subsystem (27a) exists a unique solution $Z(t) \in \mathcal{C}^1([0,+\infty) : \mathcal{R}^n)$. Similarly, we obtain that the subsystem consisting of (27e)–(27f) exists a unique solution $\tilde{\rho} \in \mathcal{C}^1([0,+\infty) : \mathcal{R}^m)$, $Q^{-1} \in \mathcal{C}^1([0,+\infty) : \mathcal{R}^{m\times m})$, that is, the subsystem consisting of (21a)–(21b) exists a unique solution $\hat{\rho} \in \mathcal{C}^1([0,+\infty) : \mathcal{R}^m)$, $Q \in \mathcal{C}^1([0,+\infty) : \mathcal{R}^{m\times m})$. Then, it is easy to verify that the subsystem consisting of (27b)–(27d) has a strong solution $w(\sigma,t) \in \mathcal{H}^1(0,\ell)$ by means of the similar analysis of *Step* 2.

Second, utilizing the usual existence theorems for ODEs, we obtain the plant (10) exists a unique solution $\lambda_{11}(t) \in \mathcal{C}^1([0,+\infty) : \mathcal{R}^{n\times m_1})$, $\lambda_{12}(t) \in \mathcal{C}^1([0,+\infty) : \mathcal{R}^{n\times m_2})$, $\lambda_{13}(t) \in \mathcal{C}^1([0,+\infty) : \mathcal{R}^{n\times m_3})$, $\lambda_{14}(t) \in \mathcal{C}^1([0,+\infty) : \mathcal{R}^{n\times m_4})$. Then, it is easy to give that the first two equations of (15) and (19) have strong solution $\lambda_{21}(\sigma,t) \in \mathcal{H}^1(0,\ell)$ and $\lambda_{22}(\sigma,t) \in \mathcal{H}^1(0,\ell)$ applying the similar method with *Step* 2. Next, applying the method of separation of variables (see Ref. [27]), it follows that the last two equations of (15) and (19) have closed-loop solution.

The above analysis implies that the plant consisting of (5a)–(5d) exists a unique solution $\tilde{X} \in \mathcal{C}^1([0,+\infty) : \mathcal{R}^n)$ and $\tilde{u}(\sigma,t) \in \mathcal{H}^1(0,\ell)$, due to (6a)–(6b). Consequently, the similar results for the observer states $\hat{X}(t)$ and $\hat{u}(\sigma,t)$ are hold.

## Appendix C: The proof of Lemma 1

From (10), we found that $\lambda_{1i}(t)(i = 1,2,3,4)$ are bounded if $\lambda_{2i}(0,t)(i = 1,2,3,4)$ are bounded, due to the signal $\phi_1(t)$ is bounded and $A - LC\Omega^{-1}(\ell)$ is a Hurwitz matrix. Therefore, we only need to suggest $\lambda_{2i}(\sigma,t)(i = 1,2,3,4)$ are bounded. Consider the ensuing Lyapunov functional

$$W_{21}(t) = \frac{1}{2}\int_0^\ell \lambda_{21}(\sigma,t)\lambda_{21}^T(\sigma,t)d\sigma + \frac{1}{2}\int_0^\ell \lambda_{21,\sigma}(\sigma,t)\lambda_{21,\sigma}^T(\sigma,t)d\sigma. \quad \text{(C.1)}$$

Differentiating (C.1) and applying the integration by parts formula, it follows from the first equation of (15) and (19) that

$$\begin{aligned}\dot{W}_{21}(t) =& \int_0^\ell \lambda_{21}(\sigma,t)\lambda_{21,t}^T(\sigma,t)d\sigma \\ &+ \int_0^\ell \lambda_{21,\sigma}(\sigma,t)\lambda_{21,\sigma t}^T(\sigma,t)d\sigma \\ =& -h\int_0^\ell \lambda_{21,\sigma}(\sigma,t)\lambda_{21,\sigma}^T(\sigma,t)d\sigma \\ &- \int_0^\ell \lambda_{21}(\sigma,t)\big(C\Omega(\sigma)\Omega^{-1}(\ell)\phi_1(t)\big)^T d\sigma \\ &- h\int_0^\ell \lambda_{21,\sigma\sigma}(\sigma,t)\lambda_{21,\sigma\sigma}^T(\sigma,t)d\sigma \\ &+ \int_0^\ell \lambda_{21,\sigma\sigma}(\sigma,t)\big(C\Omega(\sigma)\Omega^{-1}(\ell)\phi_1(t)\big)^T d\sigma. \end{aligned} \quad \text{(C.2)}$$

Then, by means of Young's inequality for (C.2), we get

$$\begin{aligned}\dot{W}_{21}(t) =& -h\int_0^\ell \|\lambda_{21,\sigma}(\sigma,t)\|^2 d\sigma \\ &+ \frac{\eta}{2}\int_0^\ell \|\lambda_{21}(\sigma,t)\|^2 d\sigma \\ &+ \frac{1}{2\eta}\int_0^\ell \|C\Omega(\sigma)\Omega^{-1}(\ell)\phi_1(t)\|^2 d\sigma \\ &- \Big(h - \frac{\zeta}{2}\Big)\int_0^\ell \|\lambda_{21,\sigma\sigma}(\sigma,t)\|^2 d\sigma \\ &+ \frac{1}{2\zeta}\int_0^\ell \|C\Omega(\sigma)\Omega^{-1}(\ell)\phi_1(t)\|^2 d\sigma, \end{aligned}$$

where $\eta$ and $\zeta$ are positive scalars to be determined later. Then, applying (1a) yields

$$\begin{aligned}\dot{W}_{21}(t) \leq& -\Big(h - \frac{2\eta\ell^2}{\pi^2}\Big)\int_0^\ell \|\lambda_{21,\sigma}(\sigma,t)\|^2 d\sigma \\ &+ \Big(\frac{1}{2\eta} + \frac{1}{2\zeta}\Big)\int_0^\ell \|C\Omega(\sigma)\Omega^{-1}(\ell)\phi_1(t)\|^2 d\sigma \\ &- \Big(h - \frac{\zeta}{2}\Big)\int_0^\ell \|\lambda_{21,\sigma\sigma}(\sigma,t)\|^2 d\sigma. \end{aligned}$$

Taking positive constants $\eta < \frac{\pi^2 h}{2\ell^2}$ and $\zeta < 2h$, clearly, we have

$$h - \frac{2\eta\ell^2}{\pi^2} > 0, \quad h - \frac{\zeta}{2} > 0.$$

Then, by means of Wirtinger's inequality (1a) again, we obtain

$$\begin{aligned}\dot{W}_{21}(t) \leq & -\Big(h - \frac{2\eta\ell^2}{\pi^2}\Big)\frac{\pi^2}{4\ell^2}\int_0^\ell \|\lambda_{21}(\sigma,t)\|^2 d\sigma \\ & +\Big(\frac{1}{2\eta}+\frac{1}{2\zeta}\Big)\int_0^\ell \|C\Omega(\sigma)\Omega^{-1}(\ell)\phi_1(t)\|^2 d\sigma \\ & -\Big(h - \frac{\zeta}{2}\Big)\frac{\pi^2}{4\ell^2}\int_0^\ell \|\lambda_{21,\sigma}(\sigma,t)\|^2 d\sigma \\ \leq & \Big(\frac{1}{2\eta}+\frac{1}{2\zeta}\Big)\int_0^\ell \|C\Omega(\sigma)\Omega^{-1}(\ell)\phi_1(t)\|^2 d\sigma \\ & -\frac{\pi^2}{2\ell^2}\min\Big\{h - \frac{2\eta\ell^2}{\pi^2}, h - \frac{\zeta}{2}\Big\} W_{21}(t).\end{aligned}$$

It can be obtained that $W_{21}(t)$ is bounded, due to the signal $\phi_1(t)$ and matrix function $\Omega(\sigma)$ are bounded. (C.1) implies that $\int_0^\ell \|\lambda_{21}(\sigma,t)\|^2 d\sigma$ and $\int_0^\ell \|\lambda_{21,\sigma}(\sigma,t)\|^2 d\sigma$ are bounded. From (1b), we infer that $\|\lambda_{21}(\sigma,t)\|$ is bounded, so is $\|\lambda_{11}(t)\|$.

In the same manner, we can infer that $\|\lambda_{22}(\sigma,t)\|$, $\|\lambda_{23}(\sigma,t)\|$ and $\|\lambda_{24}(\sigma,t)\|$ are bounded, which suggest that $\|\lambda_{12}(t)\|$, $\|\lambda_{13}(t)\|$ and $\|\lambda_{14}(t)\|$ are also bounded.

## References


1. Smyshlyaev, A., Krstic, M.: Backstepping observers for a class of parabolic PDEs. Syst. Control Lett. **54**(7), 613–625 (2005)
2. Tang, S., Xie, C.: State and output feedback boundary control for a coupled PDE-ODE system. Syst. Control Lett. **60**(8), 540–545 (2011)
3. Li, J., Liu, Y.: Stabilization of coupled PDE-ODE systems with spatially varying coefficient. J. Syst. Sci. Complex. **26**, 151–174 (2013)
4. Wu, H.N., Wang, J.W.: Observer design and output feedback stabilization for nonlinear multivariable systems with diffusion PDE-governed sensor dynamics. Nonlinear Dyn. **72**(3), 615–628 (2013)
5. Hasan, A., Aamo, O.M., Krstic, M.: Boundary observer design for hyperbolic PDE-ODE cascade systems. Automatica **68**, 75–86 (2016)
6. Mathiyalagan, K., Nidhi, A.S., Su, H., Renugadevi, T.: Observer and boundary output feedback control for coupled ODE-transport PDE. Appl. Math. Comput. **426**, 127096 (2022)
7. Mathiyalagan, K., Nidhi, A.S.: Observer and output feedback control for nonlinear ordinary differential equation coupled to an under-actuated transport partial differential equation. Int. J. Robust Nonlinear Control **32**(12), 7074–7098 (2022)
8. Krstic, M.: Compensating actuator and sensor dynamics governed by diffusion PDEs. Syst. Control Lett. **58**(5), 372–377 (2009)
9. Ahmed-Ali, T., Giri, F., Krstic, M., Lamnabhi-Lagarrigue, F.: Observer design for a class of nonlinear ODE-PDE cascade systems. Syst. Control Lett. **83**, 19–27 (2015)
10. Ahmed-Ali, T., Giri, F., Krstic, M., Kahelras, M.: PDE based observer design for nonlinear systems with large output delay. Syst. Control Lett. **113**, 1–8 (2018)
11. Ahmed-Ali, T., Giri, F., Karafyllis, I., Krstic, M.: Sampled boundary observer for strict-feedback nonlinear ODE systems with parabolic PDE sensor. Automatica **101**, 439–449 (2019)
12. Benabdelhadi, A., Lailler, M., Giri, F., Ahmed-Ali, T., Fadil, H.E.I., Chaoui, F.: Sampled-output observer design in the presence of nonlinear heat PDE sensor. Int. J. Control **95**(3), 743–752 (2022)
13. Koga, S., Krstic, M.: State estimation of the Stefan PDE: a tutorial on design and applications to polar ice and batteries. Annu. Rev. Control **53**, 199–223 (2022)
14. Smyshlyaev, A., Krstic, M.: Adaptive control of parabolic PDEs, Princeton, NJ. Princeton University Press, USA (2010)
15. Ahmed-Ali, T., Giri, F., Krstic, M., Burlion, L., Lamnabhi-Lagarrigue,, F.: Adaptive observer for parabolic PDEs with uncertain parameter in the boundary condition. In: 2015 European Control Conference (ECC), pp. 1343–1348 (2015)
16. Ahmed-Ali, T., Giri, F., Krstic, M., Burlion, L., Lamnabhi-Lagarrigue, F.: Adaptive boundary observer for parabolic PDEs subject to domain and boundary parameter uncertainties. Automatica **72**, 115–122 (2016)
17. Ji, C., Zhang, Z.: Adaptive boundary observer design for coupled parabolic PDEs with different diffusions and parameter uncertainty. IEEE Trans. Circuits Syst. I Reg. Pap. **69**(7), 3037–3047 (2022)
18. Ghousein, M., Witrant, E., Bhanot, V., Petagna, P.: Adaptive boundary observer design for linear hyperbolic systems, application to estimation in heat exchangers. Automatica **114**, 108824 (2020)
19. Benabdelhadi, A., Giri, F., Ahmed-Ali, T., Krstic, M., Chaoui, F.Z.: Adaptive observer design for wave PDEs with nonlinear dynamics and parameter uncertainty. Automatica **123**(5), 109295 (2021)
20. Ahmed-Ali, T., Giri, F., Krstic, M., Burlion, L., Lamnabhi-Lagarrigue, F.: Adaptive observer design with heat PDE sensor. Automatica **82**, 93–100 (2017)
21. Wen, Y., Lou, X., Wu, W., Cui, B.: Impulsive adaptive observer design for a class of hybrid ODE-PDE cascade systems with uncertain parameters. Syst. Control Lett. **154**, 104969 (2021)
22. Hardy, G., Littlewood, J., Polya, G.: Inequalities. Cambridge University Press, Cambridge, UK (1934)
23. Fridman, E., Blighovsky, A.: Robust sampled-data control of a class of semilinear parabolic systems. Automatica **48**, 826–836 (2012)

24. Zhang, Q.: Adaptive observer for multiple-input-multiple-output (MIMO) linear time-varying systems. IEEE Trans. Autom. Control **47**(3), 525–529 (2002)
25. Ioannou, P.A., Sun, J.: Robust adaptive control. Prentice Hall, Upper Saddle River, NJ (2006)
26. Schaum, A., Moreno, J.A., Fridman, E., Alvarez, J.: Matrix inequality-based observer design for a class of distributed transport-reaction systems. Int. J. Robust Nonlinear Control **24**(16), 2213–2230 (2014)
27. Evans, L.C.: Partial differential equations, Rhode Island. American Mathematical Society, USA (2010)
28. Henry, D.: Geometric theory of semilinear parabolic equations. Springer, New York (1981)
29. Goodwin, G.C., Mayne, D.Q.: A parameter estimation perspective of continuous time model reference adaptive control. Automatica **23**(1), 57–70 (1987)
30. Yang, W.Y., Cao, W., Chung, T.S., Morris, J.: Applied numerical methods using MATLAB. Wiley, Hoboken, NJ (2005)
31. Abinandhitha, R., Sakthivel, R., Kong, F., Parivallal, A.: Robust non-fragile boundary control for non-linear parabolic PDE systems with semi-Markov switching and input quantization. Eur. J. Control **67**, 100713 (2022)